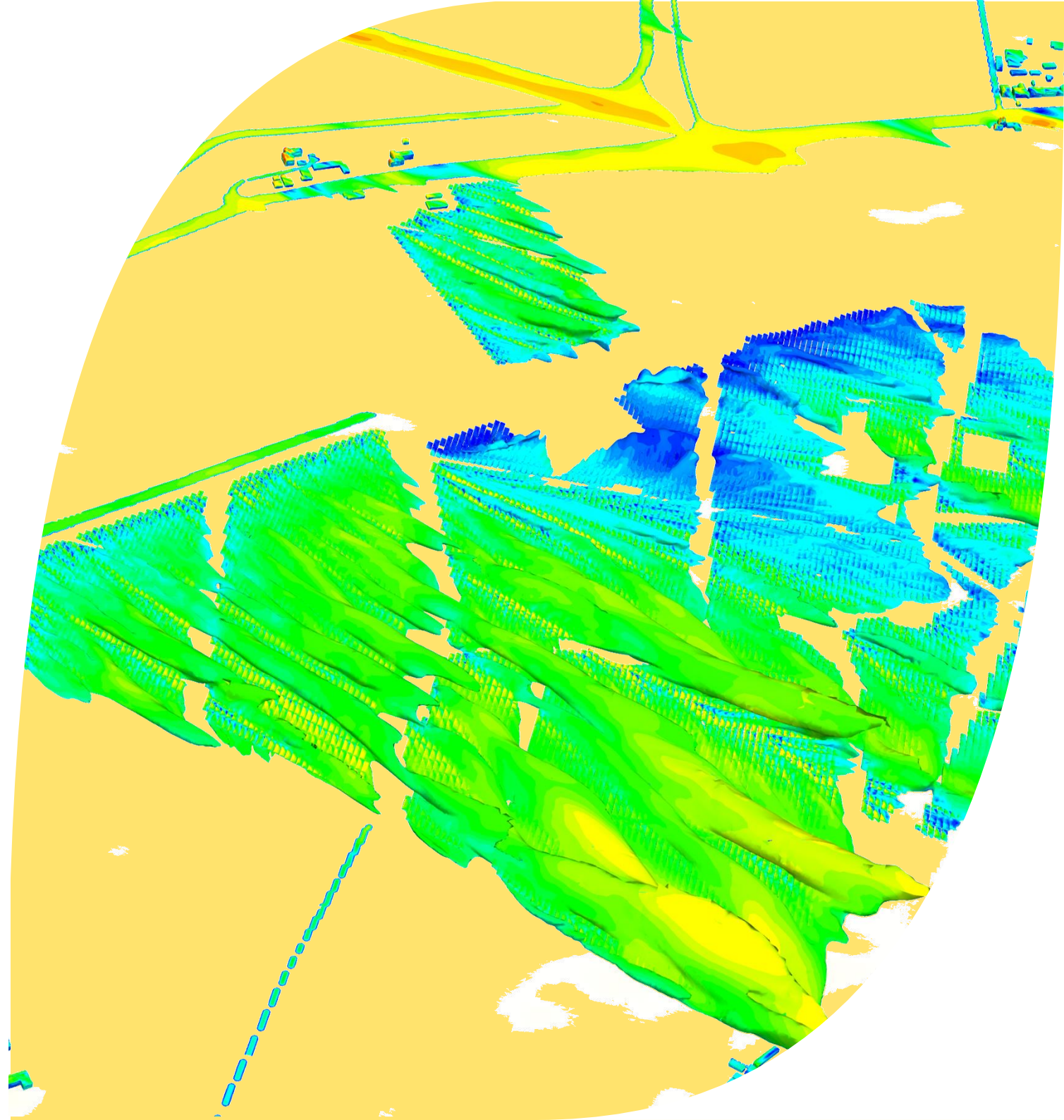


**Botley West Solar Farm
Oxford, UK**

Thermal Impact

16th October 2025




Botley West Solar Farm Oxford, UK

Thermal Impact

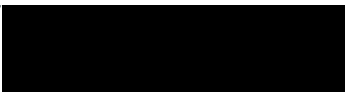
For: SolarFive Ltd

Doc. No.	Version	Date	Comments
75223rep1v1	1	16 th October 2025	First issue



Author: 

Ms A. Bagnara

Appr 

Dr D. Hankin

© Copyright NOVA Fluid Mechanics Ltd 2025
4 Vicarage Road, Teddington, England, TW11 8EZ
enquiries@novafluidmechanics.com

The information contained in this report is commercial in confidence and must not be transmitted to a third party without the prior written agreement of NOVA Fluid Mechanics Ltd.

Contents

1.	Introduction.....	4
2.	Study Area	4
3.	Assessment Methodology	5
4.	Results.....	6
5.	Conclusions	7
6.	References.....	8
APPENDIX A.	Wind Climate Analysis.....	13
APPENDIX B.	Simulation Details	17
APPENDIX C.	Contour Plots.....	29

Executive Summary

Background

A computational fluid dynamics study has been carried out by NOVA Fluid Mechanics Ltd to assess the potential thermal impact of the proposed Botley West Solar Farm development on conditions along the flight path from Runway 01 of London Oxford Airport.

The thermal impact of the proposed site along the flight path has been assessed for wind speeds based on 25%, 50% and 75% annual time exceedance, for each wind sector, for 8 critical wind directions.

Conclusions

On the basis of the numerical modelling, the following conclusions have been drawn:

- The maximum increase in air temperature associated with the thermal effect of the solar farm is 1.1 °C, with an average increase across all assessed cases of 0.6 °C.
- It is estimated that the resulting increase in exceedance of the vertical turbulence threshold commonly applied to building induced turbulence is of the order of 1.1% over the course of the year, across the assessed wind directions.

Consequently, it is expected that the impact of the proposed solar farm will be minor, and thus may not be considered significant.

Botley West Solar Farm

1. Introduction

A computational fluid dynamics study has been carried out by NOVA Fluid Mechanics Ltd to assess the potential thermal impact of the proposed Botley West Solar Farm development on conditions along the flight path from Runway 01 of London Oxford Airport.

The thermal impact of the proposed site along the flight path has been assessed for wind speeds based on 25%, 50% and 75% annual time exceedance, for each wind sector, for 8 critical wind directions.

2. Study Area

2.1. Site Location & Surrounding Area

The proposed development is located to the south-west of London Oxford Airport in the UK. The site is situated approximately 250 m to the south-west of the runway.

At present the area immediately surrounding the proposed development principally comprises open countryside interspersed with several wooded areas and villages. Oxford and its surrounding suburbs lie to the south-east.

The site location is presented within the context of the wider surrounding area in Figure 2.1.

2.2. Proposed Development

The proposed development comprises approximately 7800 photovoltaics (PV) panels, spread over an approximately 87 ha site.

3. Assessment Methodology

3.1. Wind Climate Analysis

Details of the annual wind climate analysis and wind field simulation relevant to the site are presented in Appendix A.

Based on an examination of the critical wind directions whereby the thermal effects from the proposed development have the potential to interact with the flight path, a total of eight (8) wind directions were selected for analysis, namely 22.5°, 202.5°, 225.0°, 247.5°, 270.0°, 292.5°, 315.0° and 337.5°.

The 0° wind direction has been chosen to coincide with north (90° east, 180° south, 270° west). The wind direction denotes the direction that the wind is blowing from.

Figure 3.1 presents the adopted nomenclature, along with the wind directions assessed.

3.2. Numerical Model Details

The CFD software Helyx (<https://engys.com/products/helyx>, version 4.4) was used for the thermal atmospheric boundary layer (ABL) simulations.

Details of the CFD model and numerical discretisation, along with figures of the 3D models, are presented in Appendix B.

3.3. Simulation Details

A total of 48 thermal steady state RANS ABL simulations were completed, for two site configurations, namely the proposed solar farm both with and without the thermal impact from the PV.

For each configuration, three different wind speeds, based on 25%, 50% and 75% annual time exceedance for each wind sector (at a reference height of 10 m), were modelled for 8 critical wind directions, as presented in Table 3.1.

Table 3.1: Wind speed at a reference height of 10 m

Wind Direction	25% Time Exceedance	50% Time Exceedance	75% Time Exceedance
22.5°	5.36	3.66	2.26
202.5°	5.91	4.15	2.65
225.0°	5.24	3.53	2.14
247.5°	5.55	3.73	2.25
270.0°	5.11	3.21	1.78
292.5°	5.43	3.51	2.01
315.0°	5.59	3.92	2.50
337.5°	5.59	4.02	2.64

As stipulated by the airport, it was assumed that the solar panels, along with the surrounding highways and built-up areas, are heated to 20 °C above ambient temperature, taken as the annual mean at Brize Norton from 1991-2020 of 14.6 °C^[1].

The comparison of the simulation results with and without the thermal impact of the PV enables the quantification of the thermal effect of the proposed site on the wind flow parameters in the vicinity of the airport runway.

The thermal impact has been assessed within a planar section along the runway centreline as shown in Figure 3.2.

4. Results

4.1. Results Summary

The thermal impact along the flight path is summarised as follows:

- Maximum change in the mean air temperature, see Table 4.1.

Furthermore, the results of the simulations are presented graphically in Appendix C, in terms of contour plots of the change in air temperature and change in the mean wind speed components.

4.2. Discussion

The maximum increase in air temperature associated with the thermal effect of the PV is 1.1 °C, which occurs for winds from 292.5° and 315°. Otherwise, the average increase across all cases is 0.6 °C.

For context, whilst not strictly applicable in this case, CAP 437^[2] stipulates that "...a rise of air temperature of more than 2 °C ... operational restrictions [are required]" for offshore helicopter operations. Consequently, as the indicated increase in air temperature is well below this threshold, the impacts are not expected to be significant.

In order to further quantify the potential impact of these temperature changes on flight conditions, the resulting wind velocity components have been derived, see Appendix C, and an indicative assessment of the vertical turbulence (RMS velocity) has been compared with a threshold commonly applied to building induced turbulence, namely 0.94 m/s, which corresponds to increased pilot workload during take-off / landing operations.

Whilst this approach does not account for the impact of the wind on the thermal conditions, by calculating a weighted average of the

impacts for each of the wind conditions assessed, an estimation of the likely change in the time exceedance of the aforementioned threshold can be calculated, as presented in Table 4.2.

Based on the estimated values, it is expected that the vertical turbulence associated with the thermal impact of the PV will result in an increase of the time exceedance of the threshold of the order of 1.1% over the course of the year across all wind directions assessed, with the biggest contribution once again occurring for winds from the north-western sector.

5. Conclusions

A computational fluid dynamics study has assessed the potential thermal impact of the proposed Botley West Solar Farm development on the conditions along the flight path from Runway 01 of London Oxford Airport. On the basis of the numerical modelling, the following conclusions have been drawn:

- The maximum increase in air temperature associated with the thermal effect of the solar farm is 1.1 °C, with an average increase across all assessed cases of 0.6 °C.
- It is estimated that the resulting increase in exceedance of the vertical turbulence threshold commonly applied to building induced turbulence is of the order of 1.1% over the course of the year, across the assessed wind directions.

Consequently, it is expected that the impact of the proposed solar farm will be minor, and thus may not be considered significant.

6. References

- [1] Met Office, Location-specific long-term averages. Available at: <https://www.metoffice.gov.uk/research/climate/maps-and-data/location-specific-long-term-averages/gcnyknk2h> (Accessed: 15th October 2025).
- [2] Civil Aviation Authority (2023). CAP 437: Standards for offshore helicopter landing areas.
- [3] ESDU (Engineering Science Data Unit) Item 01008. Computer Program for Wind Speeds and Turbulence Properties: Flat or Hilly Sites in Terrain with Roughness. 2001.
- [4] Menter F. (1993). Zonal Two Equation $k-\omega$ Turbulence Models for Aerodynamic Flows, AIAA Paper 93-2906.
- [5] Menter F. (2011). Turbulence Modelling for Engineering Flows, ANSYS Inc.
- [6] Richards, P.J. and Hoxey, R.P. (1993). Appropriate boundary conditions for computational wind engineering models using the $k-\epsilon$ turbulence model, Journal of Wind Engineering and Industrial Aerodynamics, vol. 46 & 47, pp. 145-153.
- [7] Manickathan, L, et al. (2017). Transpirative cooling potential of vegetation in urban environment using coupled CFD and leaf energy balance model. Proceedings of the 15th IBPSA Conference, San Francisco, CA, USA.
- [8] Dalpé, B and Masson, C. (2009). Numerical simulation of wind flow near a forest edge, Journal of Wind Engineering and Industrial Aerodynamics, Vol. 97, pp. 228-241.
- [9] Mochida, A, et al. (2008). Examining tree canopy models for CFD prediction of wind environment at pedestrian level, Journal of Wind Engineering and Industrial Aerodynamics, Vol. 96, pp. 1667-1677.

Table 4.1: Thermal impact assessment – maximum change in mean air temperature, ΔT [°C]

Wind Direction	25% Time Exceedance Wind Speeds	50% Time Exceedance Wind Speeds	75% Time Exceedance Wind Speeds
22.5°	0.05	0.64	0.52
202.5°	0.09	0.18	0.30
225.0°	0.24	0.28	0.38
247.5°	0.47	0.59	0.51
270.0°	0.87	1.03	0.66
292.5°	1.12	0.91	0.82
315.0°	1.10	0.88	0.64
337.5°	0.71	0.70	0.51

Table 4.2: Estimation of the maximum annual probability of exceedance of the vertical turbulence threshold ($\sigma_w = 0.94$ m/s)

Wind Direction	Without Thermal Load			With Thermal Load			Absolute Difference			
	25%	50%	75%	25%	50%	75%	25%	50%	75%	Total
22.5°	0.48%	0.31%	0.69%	0.48%	0.32%	0.69%	0.00%	0.01%	0.00%	0.01%
202.5°	1.58%	1.07%	1.64%	1.58%	1.07%	1.64%	0.00%	0.00%	0.00%	0.00%
225.0°	1.75%	1.20%	1.83%	1.76%	1.20%	1.83%	0.00%	0.00%	0.00%	0.00%
247.5°	2.67%	1.81%	2.74%	2.68%	1.81%	2.75%	0.00%	0.00%	0.00%	0.00%
270.0°	0.96%	0.65%	1.00%	0.96%	0.70%	1.17%	0.00%	0.05%	0.17%	0.22%
292.5°	0.54%	0.39%	0.59%	0.56%	0.44%	0.88%	0.01%	0.05%	0.29%	0.35%
315.0°	0.42%	0.35%	0.58%	0.44%	0.36%	0.72%	0.03%	0.02%	0.14%	0.19%
337.5°	0.39%	0.33%	0.56%	0.48%	0.37%	0.79%	0.09%	0.03%	0.24%	0.36%
Total:										1.13%

Figure 2.1: Aerial view of the proposed development site



Figure 3.1: Wind direction nomenclature

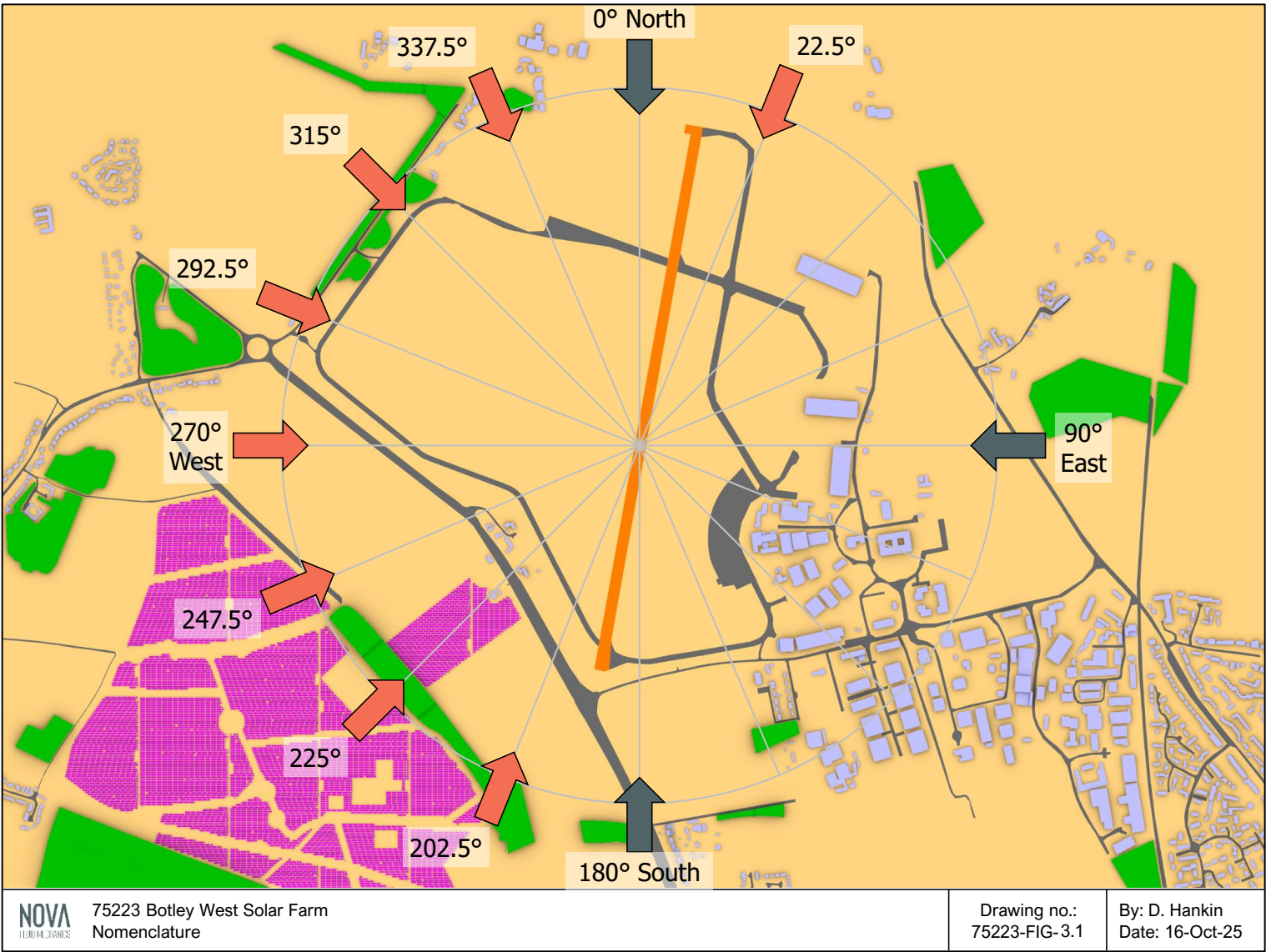
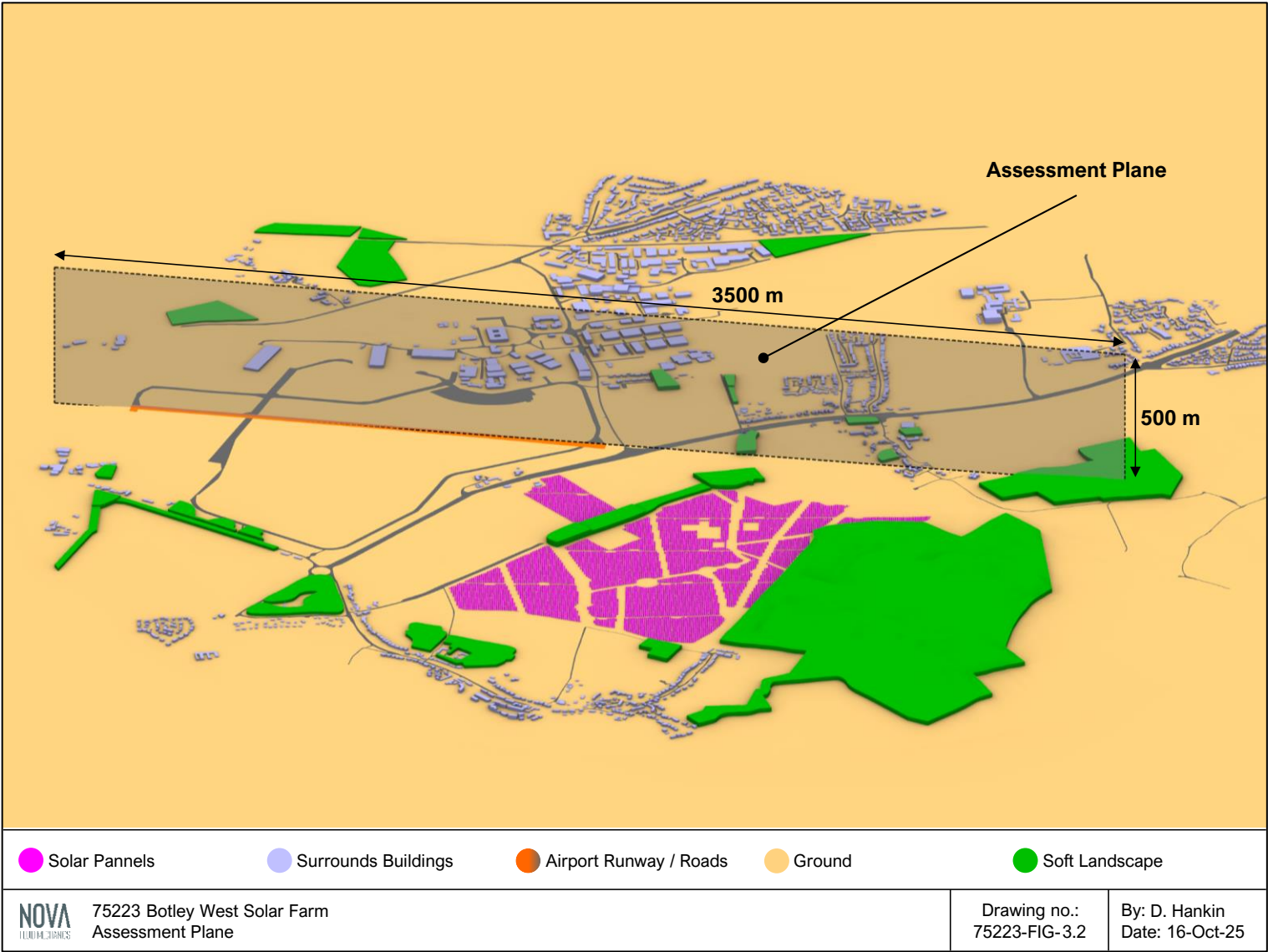


Figure 3.2: Measurement Details



APPENDIX A. WIND CLIMATE ANALYSIS

A.1. ESDU Wind Analysis

A detailed analysis was carried out to determine the wind properties at the site. The wind analysis is based on the widely accepted Deaves and Harris model of the atmospheric boundary layer (ABL), as defined in ESDU Item 01008^[3], and has provided wind profiles describing the variation of wind speed and turbulence intensity with height and wind direction. From this analysis representative profiles were defined as targets for the ABL simulation in the wind tunnel.

The wind analysis takes detailed account of the variation of the upwind terrain on each wind sector. The roughness changes used in the analysis for the current study are given in Figure A.1.

A.2. Wind Properties at the Site

Figure A.2 presents the variation of mean wind speed and longitudinal turbulence intensity used in the simulations. The wind speed profiles are normalised by the mean wind speed at the reference height of 10 m.

A.3. Wind Frequency Data

The wind speed history, provided by weather centres such as the UK Met Office or the National Oceanic & Atmospheric Administration, is reformatted into the number of observations of mean hourly wind speeds within each of several wind speed ranges, for each wind direction and for each month of the year.

To facilitate the transposition of the wind data a Weibull distribution is fitted to the wind speed distribution for each wind direction, on an annual basis.

From the Weibull cumulative distribution, the probability that, for a given wind direction, a wind speed, V , will be exceeded is given by:

$$P(> V) = e^{-\left(\frac{V}{c}\right)^k}$$

where c is the dispersion parameter and k is the shape parameter.

To these parameters is further added the probability, p , of each wind direction occurring. Thus, the probability that a specified wind speed is exceeded for a specified wind direction may be calculated.

The resulting weather centre wind data is transposed to a standard reference terrain category, 'open country terrain', at sea-level, accounting for upwind terrain, topography and altitude for the weather centre.

The open country wind data is then transposed to the reference height at the site of the proposed development, accounting for upwind terrain, topography, and altitude at the target site. The resulting annual directional and wind speed probability distributions at the reference height of 10 m, at the proposed site, are given in Figure A.3.

Values of p , c and k for the Brize Norton weather centre, being the closest station to the site with a suitable database of records, transposed to open-country terrain at 10 m height above sea-level altitude are given in Table A.1.

Figure A.1: Terrain Roughness Changes from the Site

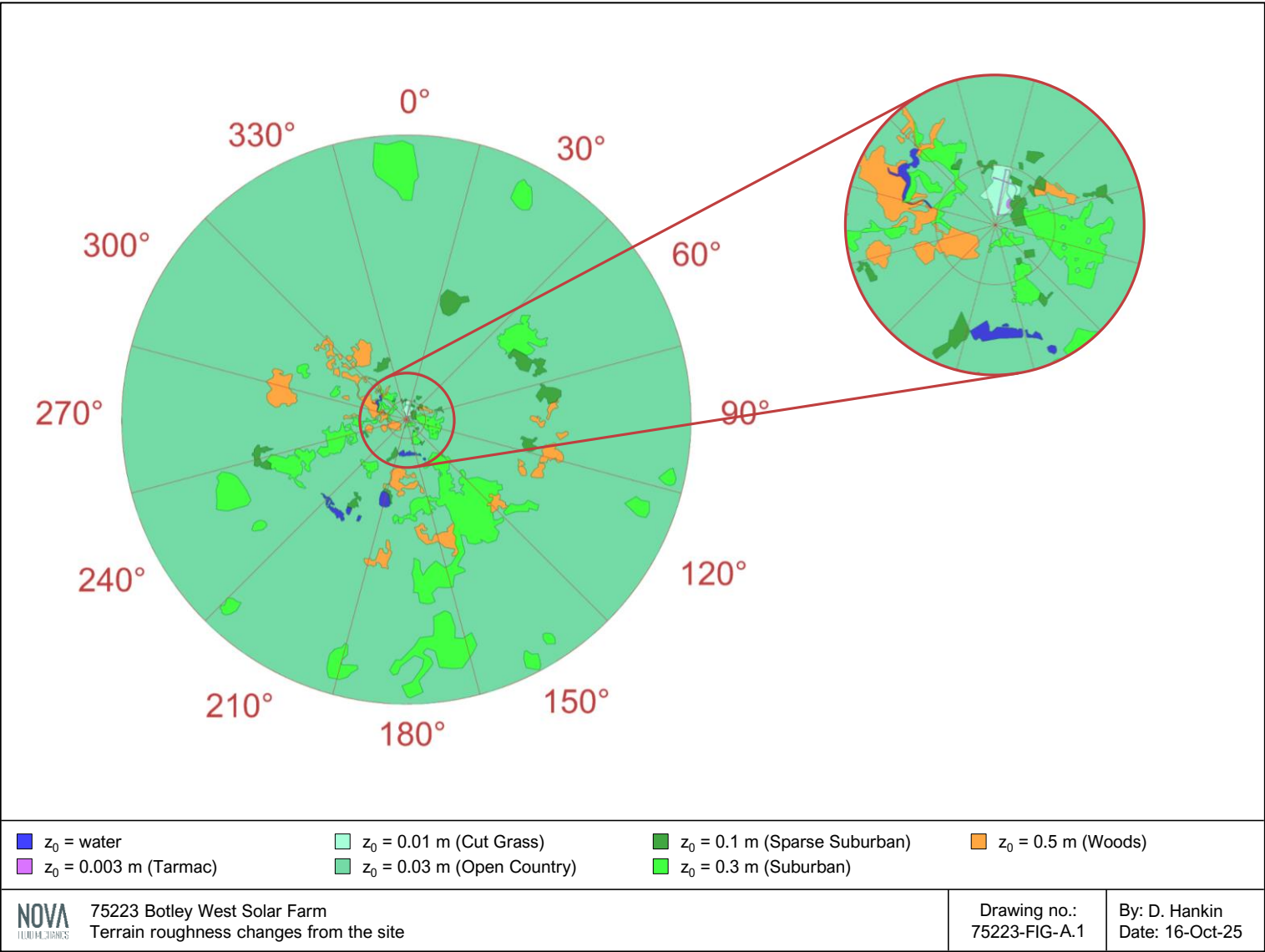


Figure A.2: Mean wind speed ($U_{\text{mean}}/U_{\text{ref}}$) and longitudinal turbulence intensity profiles (I_u) modelled in the study

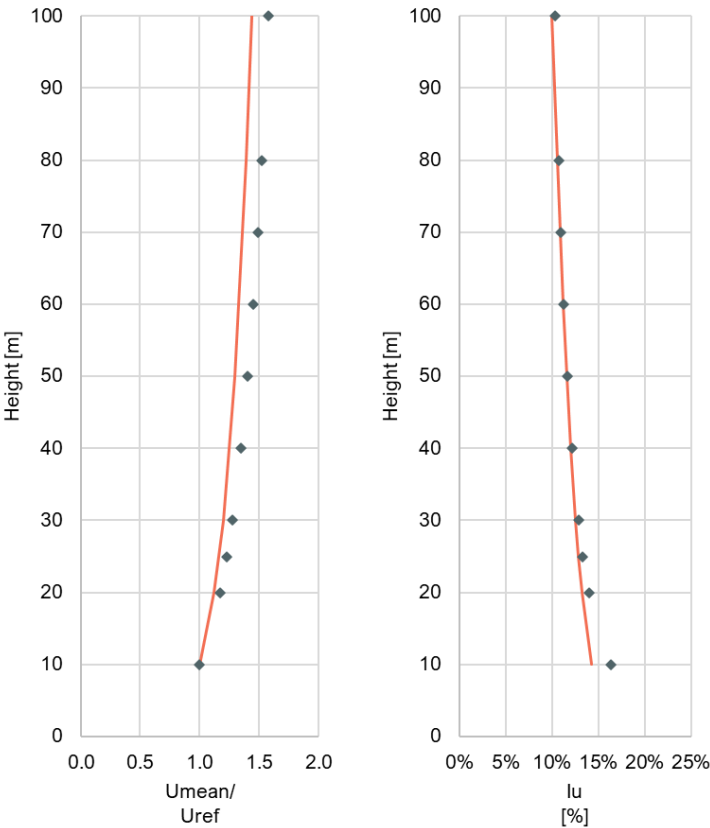


Figure A.3: Annual directional wind speed probability distribution at site (at 10 m height)

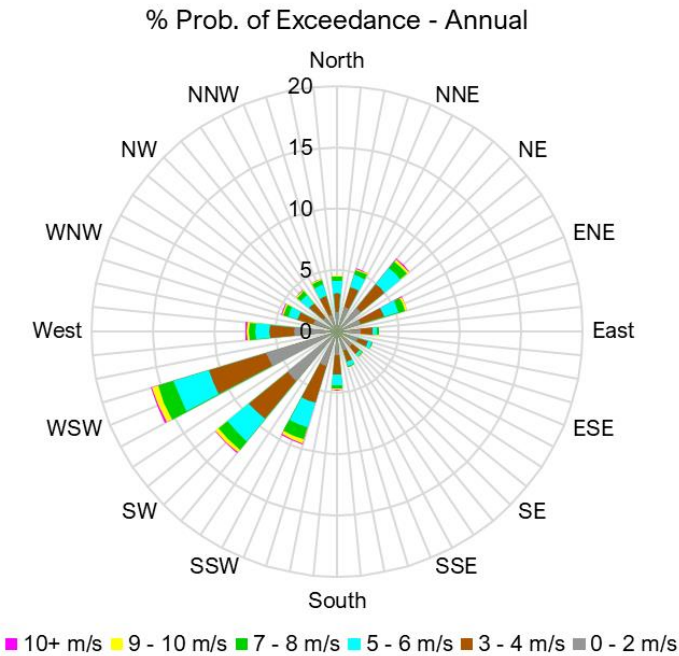


Table A.1: Wind frequency statistics: corrected Brize Norton weather centre data transposed to $z_0=0.03$ m.

Annual	0°	22.5°	45°	67.5°	90°	112.5°	135°	157.5°	180°	202.5°	225°	247.5°	270°	292.5°	315°	337.5°
p	4.56	5.35	7.64	5.99	3.45	3.01	2.71	3.06	4.82	9.62	12.86	15.89	7.45	4.76	4.37	4.47
c	4.69	4.48	4.85	4.74	3.43	3.23	3.20	3.43	4.25	5.00	4.35	4.60	4.11	4.42	4.73	4.78
k	2.02	1.82	1.95	1.92	1.56	1.77	1.74	1.68	1.81	1.96	1.76	1.74	1.49	1.58	1.95	2.09

APPENDIX B. SIMULATION DETAILS

B.1. Information for Model Construction

The model of the site was constructed based on the drawing “250602 Botley West_Middle_1 660W Masterplan_Option 2.dwg”, received 9th June 2025, and the proposed development based on the drawing “250904 Botley West Install Area Middle_1.dwg”, received 5th September 2025, both supplied by Pager Power.

The proximity model of the surrounding area was based on a site survey conducted by NOVA using publicly available information.

The models were reviewed and approved by the design team, prior to modelling.

Images of the CFD 3D model are presented as follows:

- Figure B.1: Proposed in Existing – North View
- Figure B.2: Proposed in Existing – South View
- Figure B.3: Proposed in Existing – West View
- Figure B.4: Proposed in Existing – East View
- Figure B.5: Close-up of Proposed in Existing – North View
- Figure B.6: Close-up of Proposed in Existing – South View
- Figure B.7: Close-up of Proposed in Existing – West View
- Figure B.8: Close-up of Proposed in Existing – East View

B.2. Spatial discretisation

The spatial discretisation of the 3D model was completed with the helyxHexMesh utility, part of the CFD code Helyx®. A computational mesh, consisting of approximately 72 million

hexahedral and polyhedral elements, was constructed for the proposed development in existing surrounds.

The computational domain for the purpose of the ABL simulations includes the proposed development with an explicit representation of the surrounds up to 4500 m diameter, and an additional 750 m upwind ground surface to the outer boundary of the approaching wind and sky at 1000 m height from the ground forming a cylindrical domain.

The base cell size in the numerical grid was defined as 32.0 m. The refinement level increased to 0.25 m in the zone closest to the target buildings.

Images of the CFD model discretisation are presented as follows:

- Figure B.9: View of the Spatial Discretisation
- Figure B.10: Close-up View of the spatial discretisation

B.3. Solution Methods

The RANS (Reynolds-averaged Navier–Stokes) CFD simulations were performed based on the simpleFoam solver. The modelling of an incompressible fluid flow was combined with the semi-implicit method for pressure-linked equations (SIMPLE) algorithms. The resulting turbulent flow features were modelled with introduction of the Shear Stress Transport (SST) $k-\omega$ turbulence model. This model was suggested by Menter^[4] and is based on a two-equation eddy-viscosity approach, where the SST model formulation combines the use of a $k-\omega$ in the inner parts of the boundary layer, but also switches to a $k-\epsilon$ behaviour in the free-stream regions of the solutions. Further details for the selected turbulence model are provided in the work of Menter^[5].

B.4. Initial and Boundary Conditions

The atmospheric boundary layer flow was simulated by implementing a logarithmic velocity profile model presented by Richards and Hoxey^[6], with the following main assumptions:

- The vertical velocity component at the domain boundary is negligible;
- The pressure gradient and shear stress are constant.

The model implies the following equation for the mean inlet velocity at the CFD domain:

$$U(z) = \frac{U^*}{\kappa} \ln \left(\frac{z + z_0}{z_0} \right)$$

Where:

- κ - is the von Karman's constant
- z - is the distance from the ground surface in vertical direction
- z_0 - is the ground surface roughness length in meters.

The friction velocity U^* is calculated by the following equations:

$$U^* = \kappa \frac{U_{ref}}{\ln \left(\frac{z_{ref} + z_0}{z_0} \right)}$$

Where:

- z_{ref} – is the reference height in meters
- U_{ref} - is the reference velocity in m/s measured at z_{ref} .

The turbulent velocity fluctuations at the domain inlet are induced by the constant shear stress with height, maintained by the turbulent kinetic energy k equation below:

$$k(z) = \frac{U^{*2}}{\sqrt{C_\mu}}$$

Where:

- $C_\mu = 0.09$ - is the usual k - ϵ turbulence model constant.

All surface boundary conditions were modelled as smooth walls with a no-slip condition with the exception of the ground surface outside the explicit surrounds area of the domain, which was modelled as a no-slip wall boundary condition with a varying roughness length height based on the terrain analysis for the site.

B.5. Vegetation Modelling

Porous media of the existing vegetation within vicinity of the site is modelled by introduction of volumetric source terms in the momentum equation applied at multiple cell zones defined within the CFD model.

Source terms for modelling tree canopies to account for momentum and turbulence are implemented according to Manickathan et al.^[7] and the formulations for turbulence sources of Dalpé and Manson^[8] and Mochida et. al.^[9].

Figure B.1: Proposed in Existing – North View

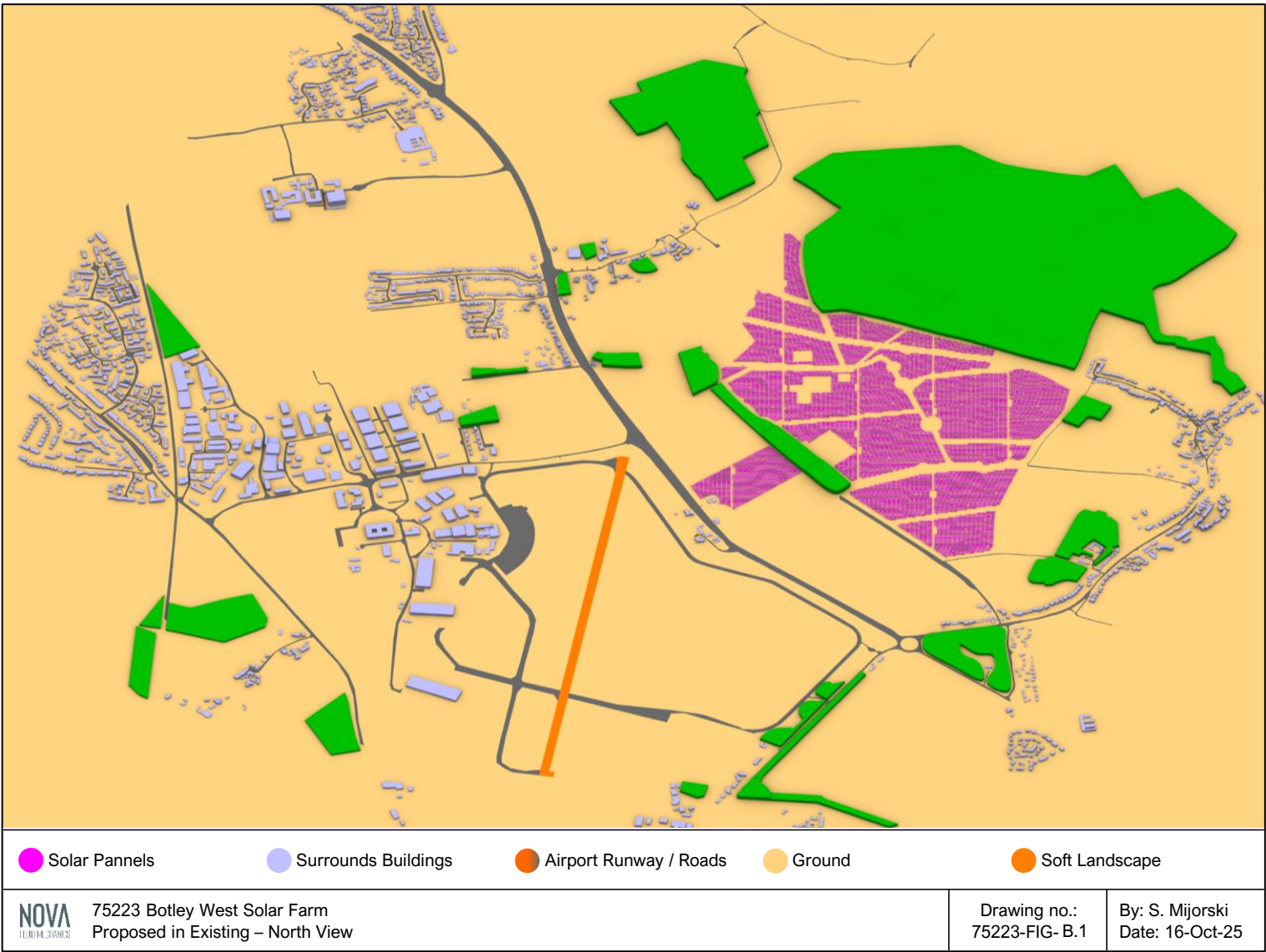


Figure B.2: Proposed in Existing – South View

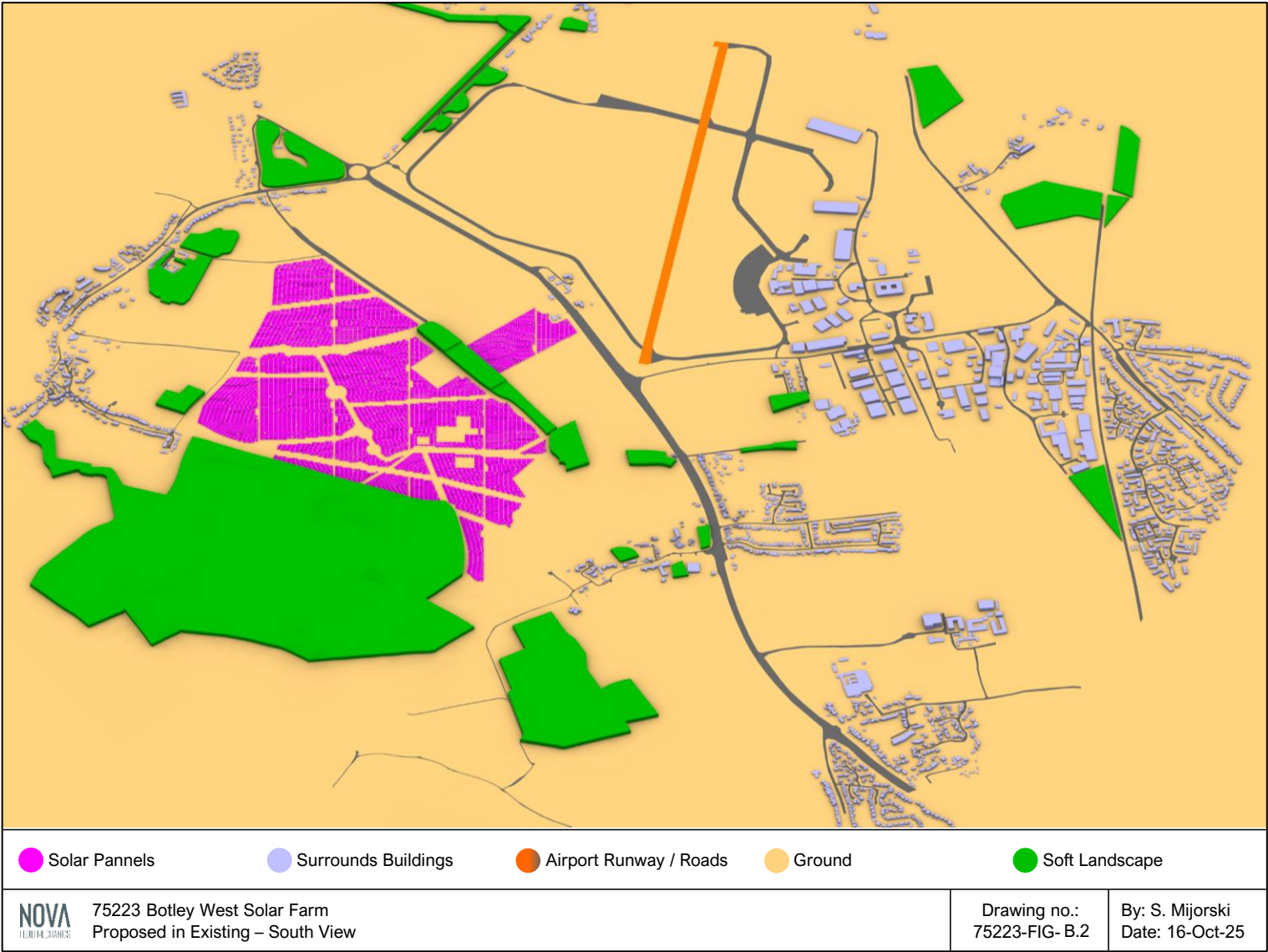


Figure B.3: Proposed in Existing – West View

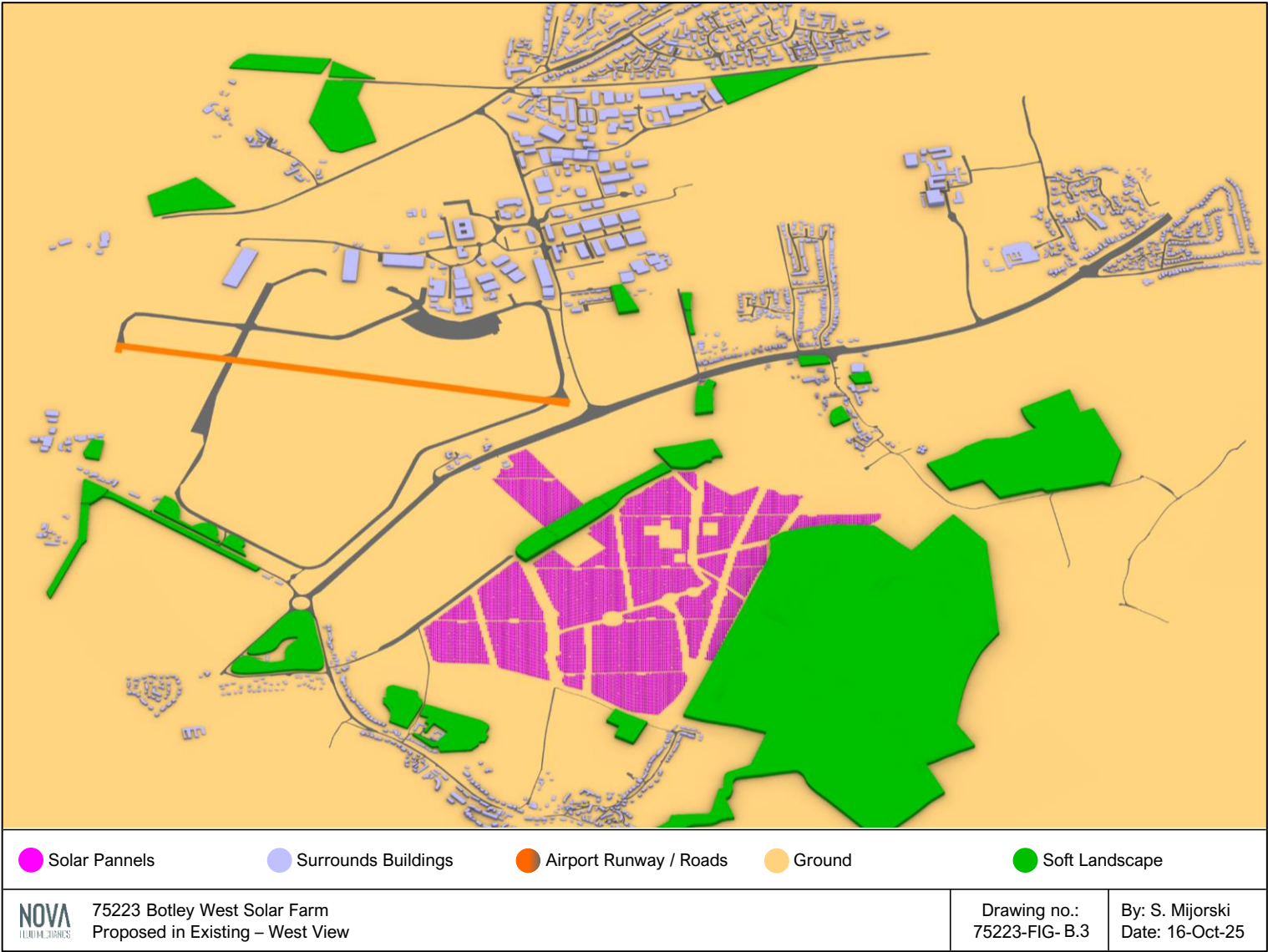


Figure B.4: Proposed in Existing – East View

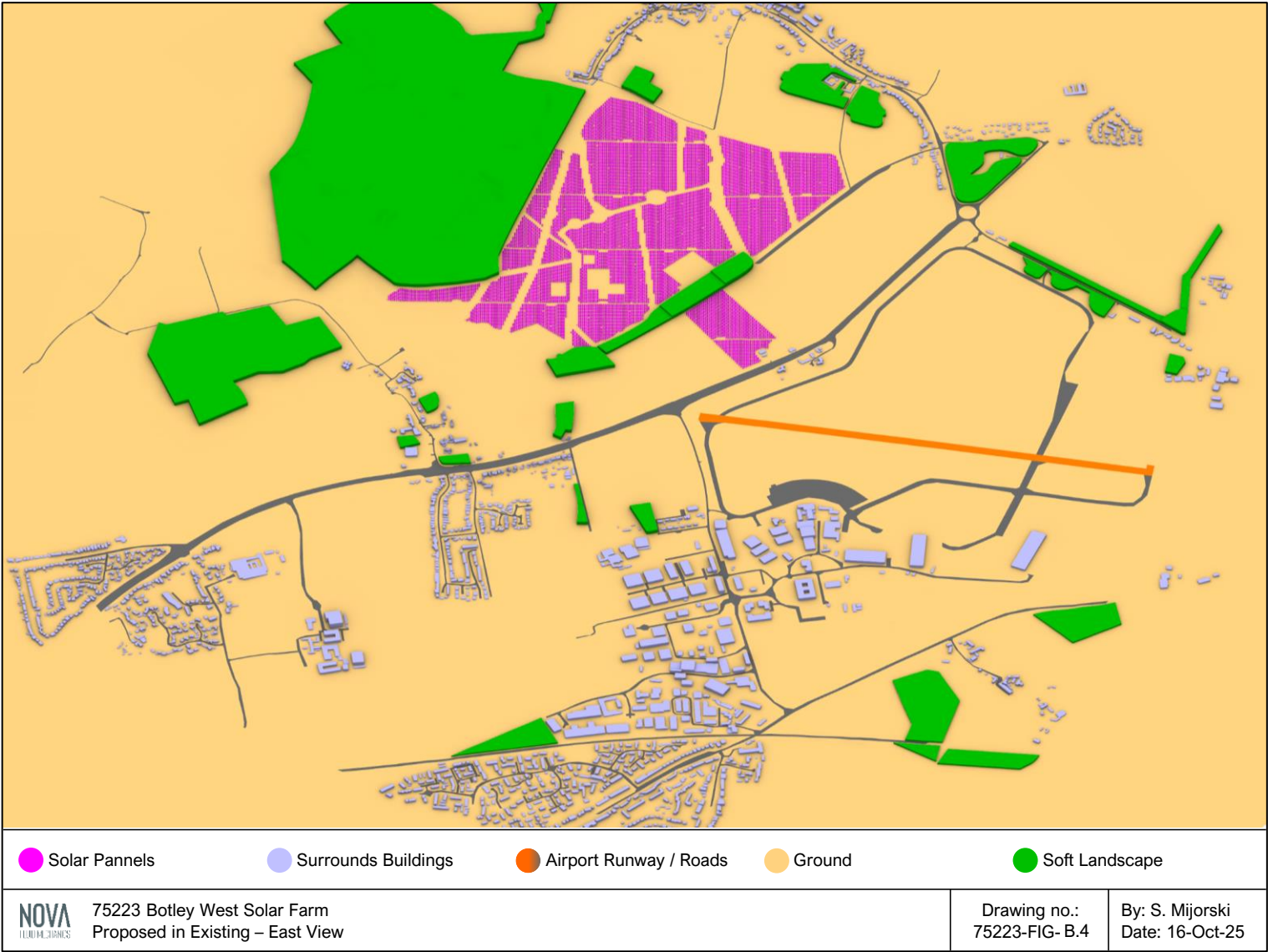


Figure B.5: Close-up of Proposed in Existing – North View

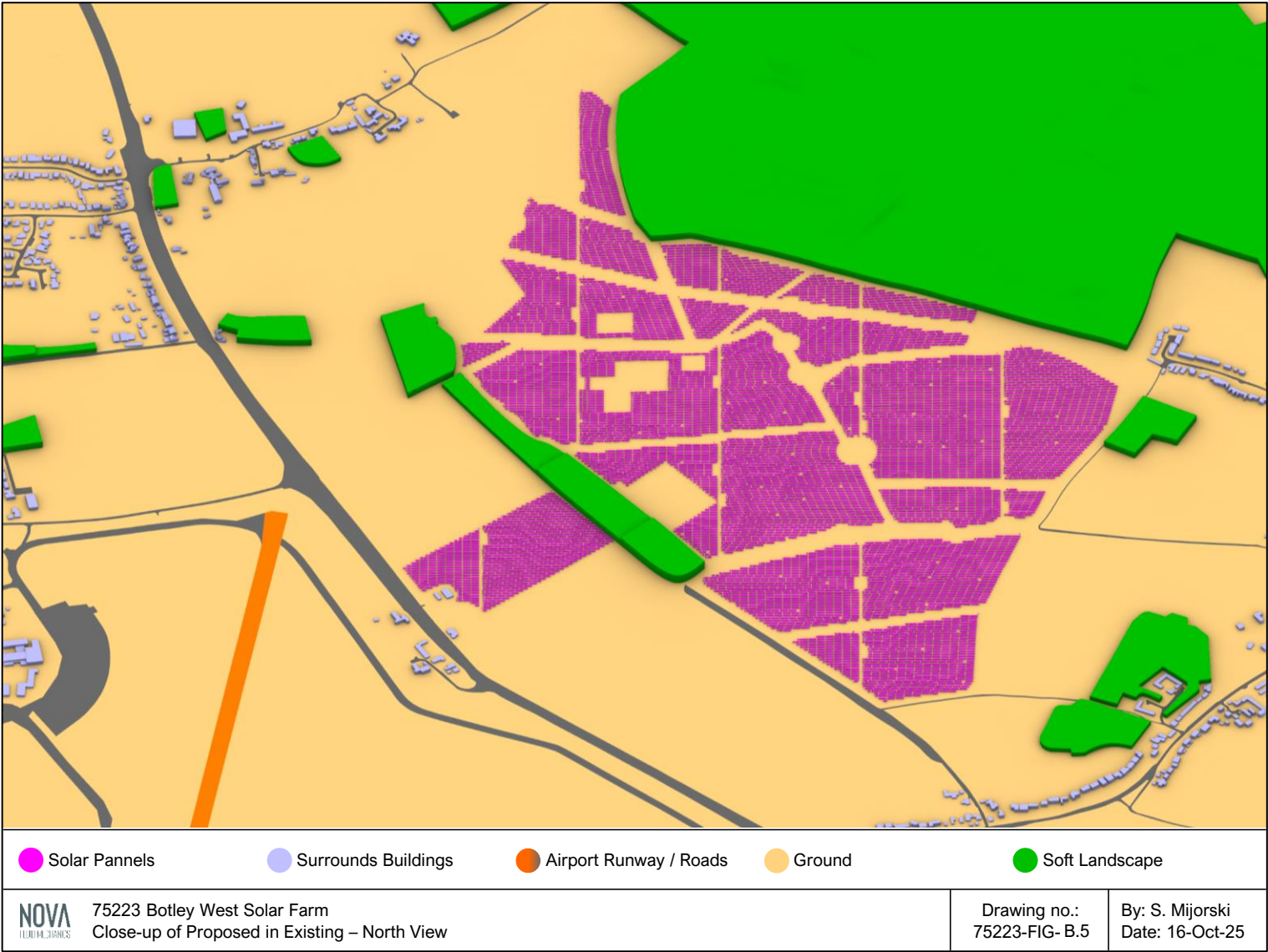


Figure B.6: Close-up of Proposed in Existing – South View

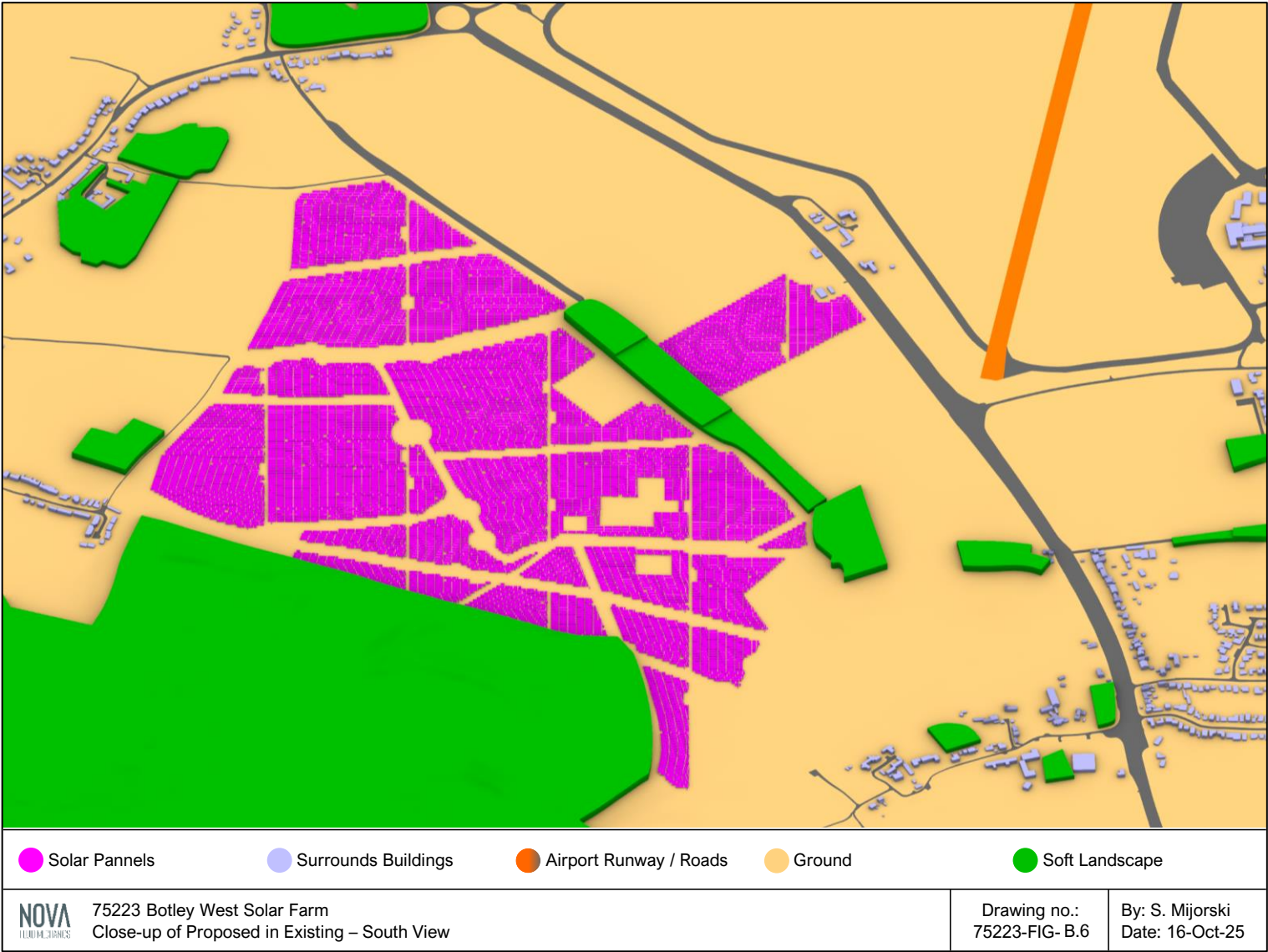


Figure B.7: Close-up of Proposed in Existing – West View

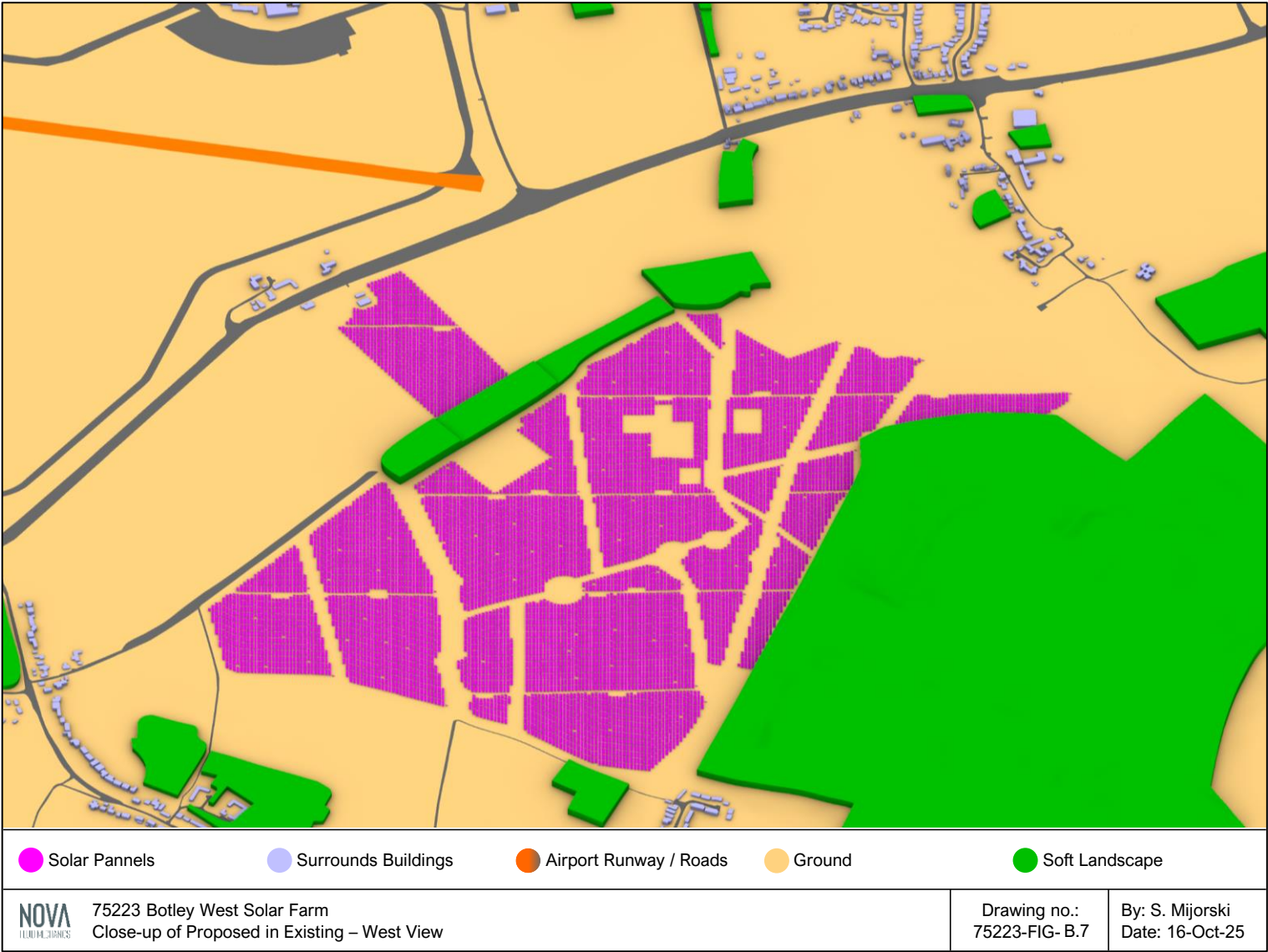


Figure B.8: Close-up of Proposed in Existing – East View

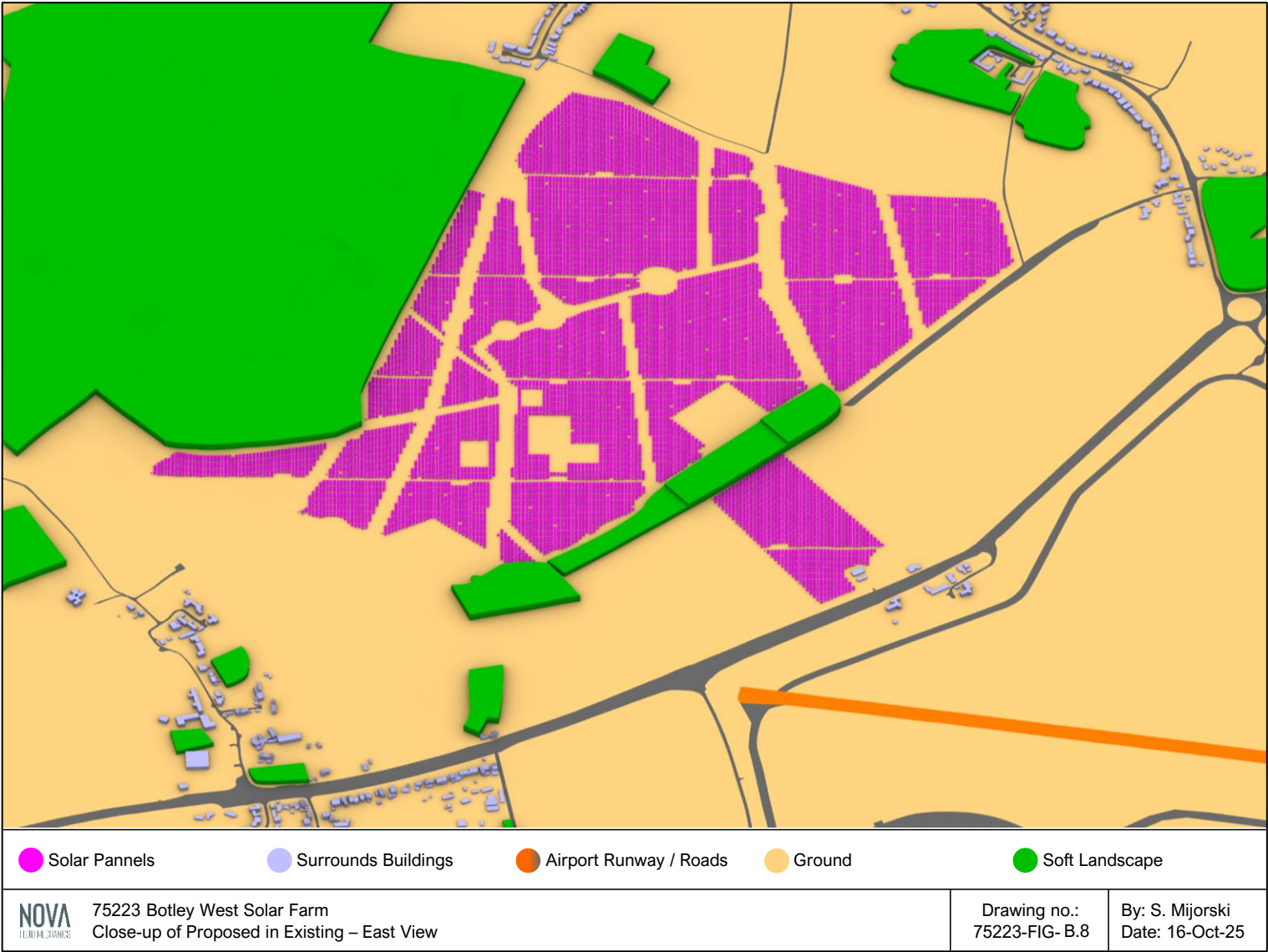


Figure B.9: View of the Spatial Discretisation

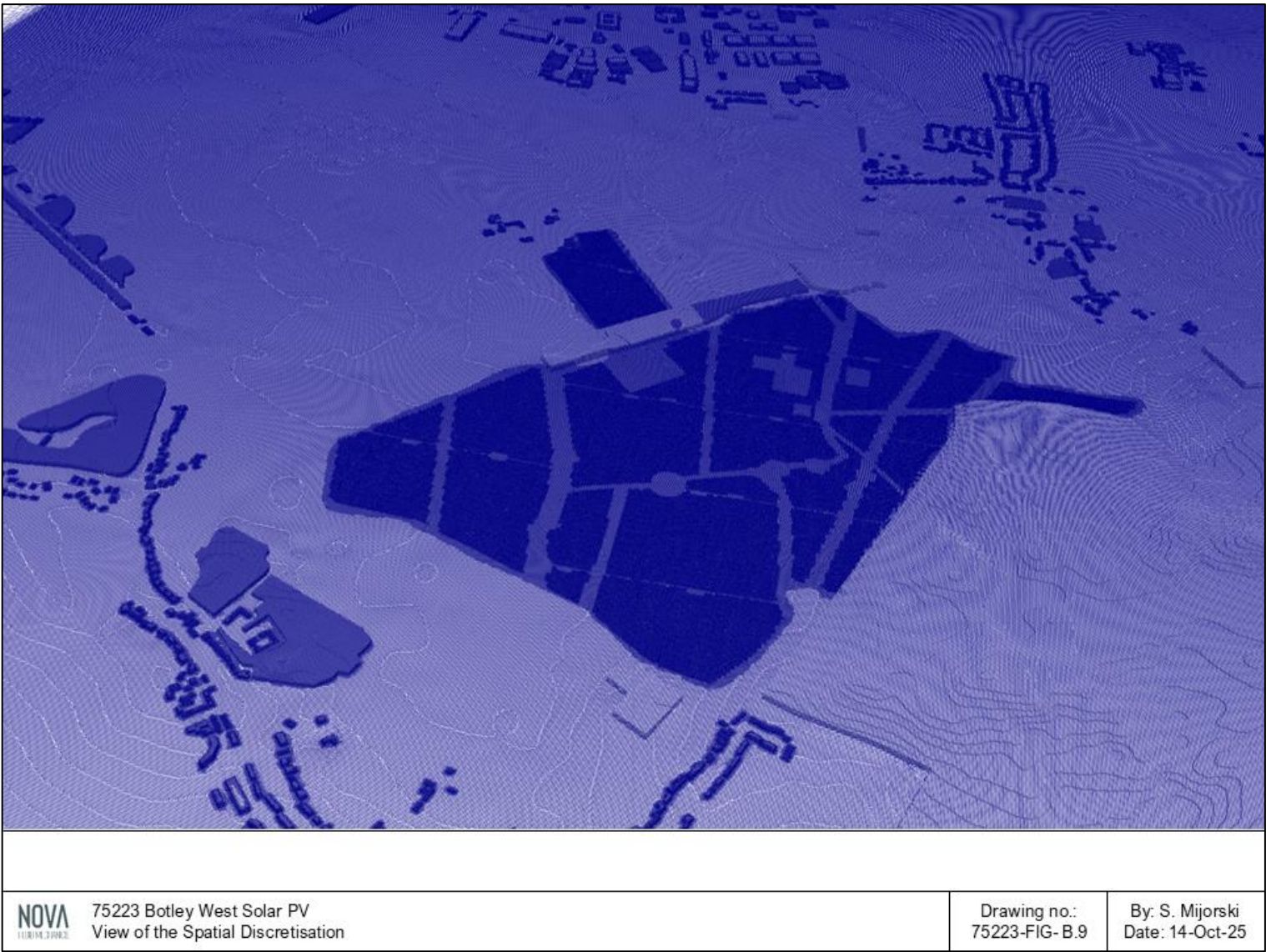
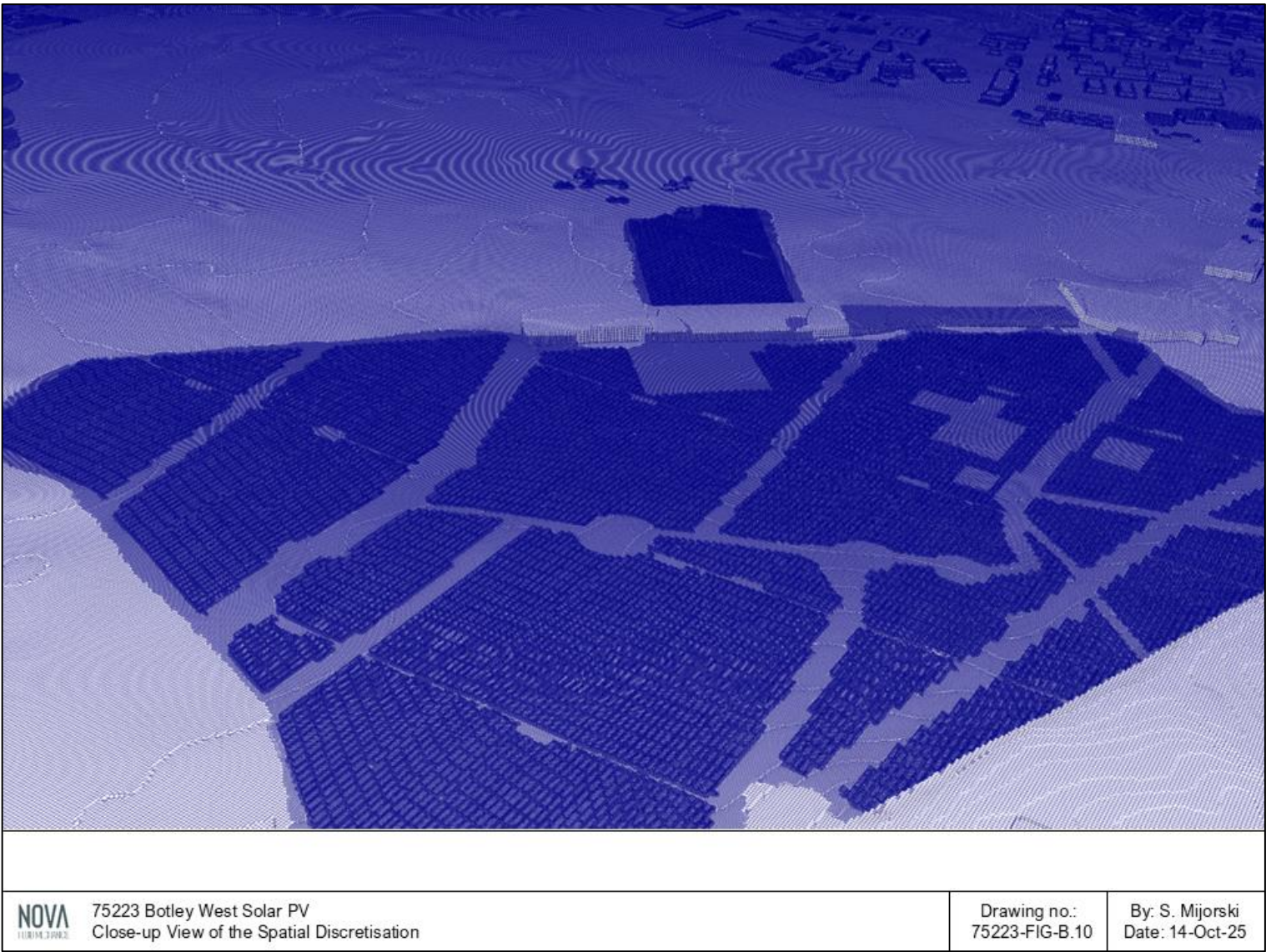


Figure B.10: Close-up View of the Spatial Discretisation



APPENDIX C. CONTOUR PLOTS

The thermal impact of the proposed development is presented graphically in Figures C.1 to C.32, in terms of contours of the change in air temperature and the change in each of the mean velocity components, for wind speeds based on 25%, 50% and 75% annual time exceedance, for each of the critical wind directions, derived from the numerical simulations.

The u-component velocities correspond to cross-winds, the v-component to winds along the runway, and the w-component to vertical winds.

It is noted that the corresponding gradient scale colouring has been selected in order to provide the maximum contrast in the results and does not in itself indicate the suitability or otherwise of conditions.

Figure C.1: Change in Air Temperature – Winds from 22.5°

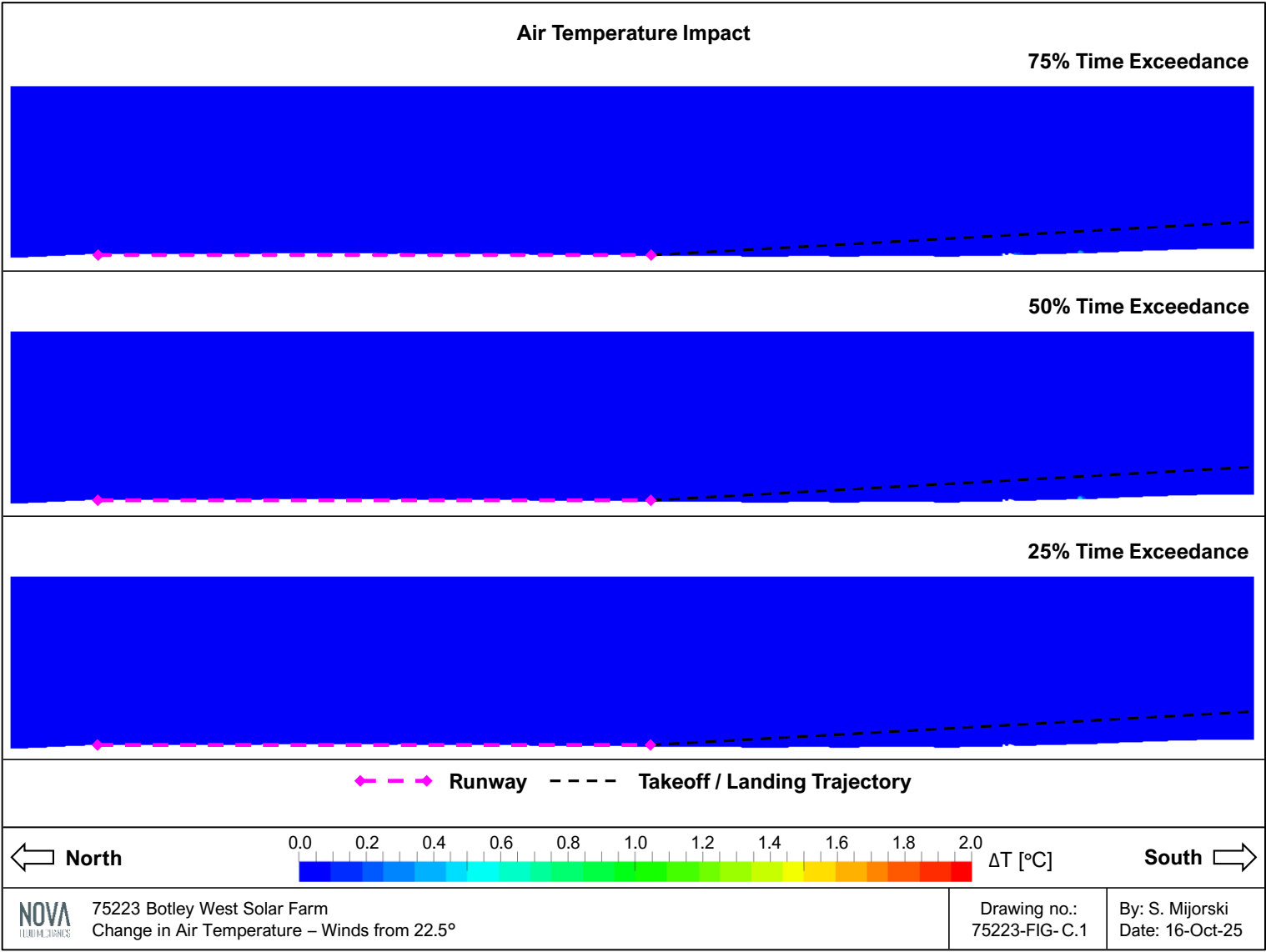


Figure C.2: Change in Mean Wind Speed – U-component – Winds from 22.5°

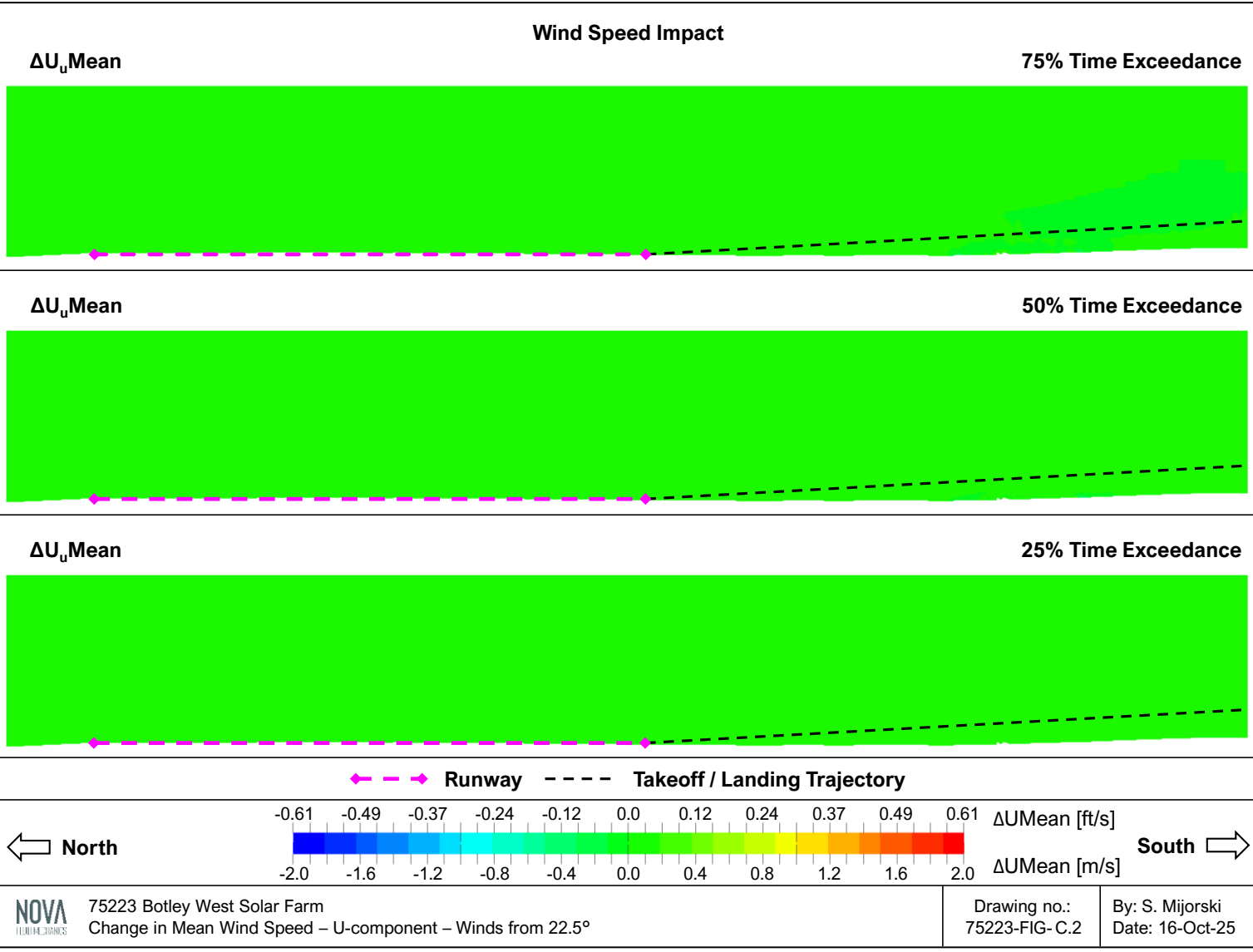


Figure C.3: Change in Mean Wind Speed – V-component – Winds from 22.5°

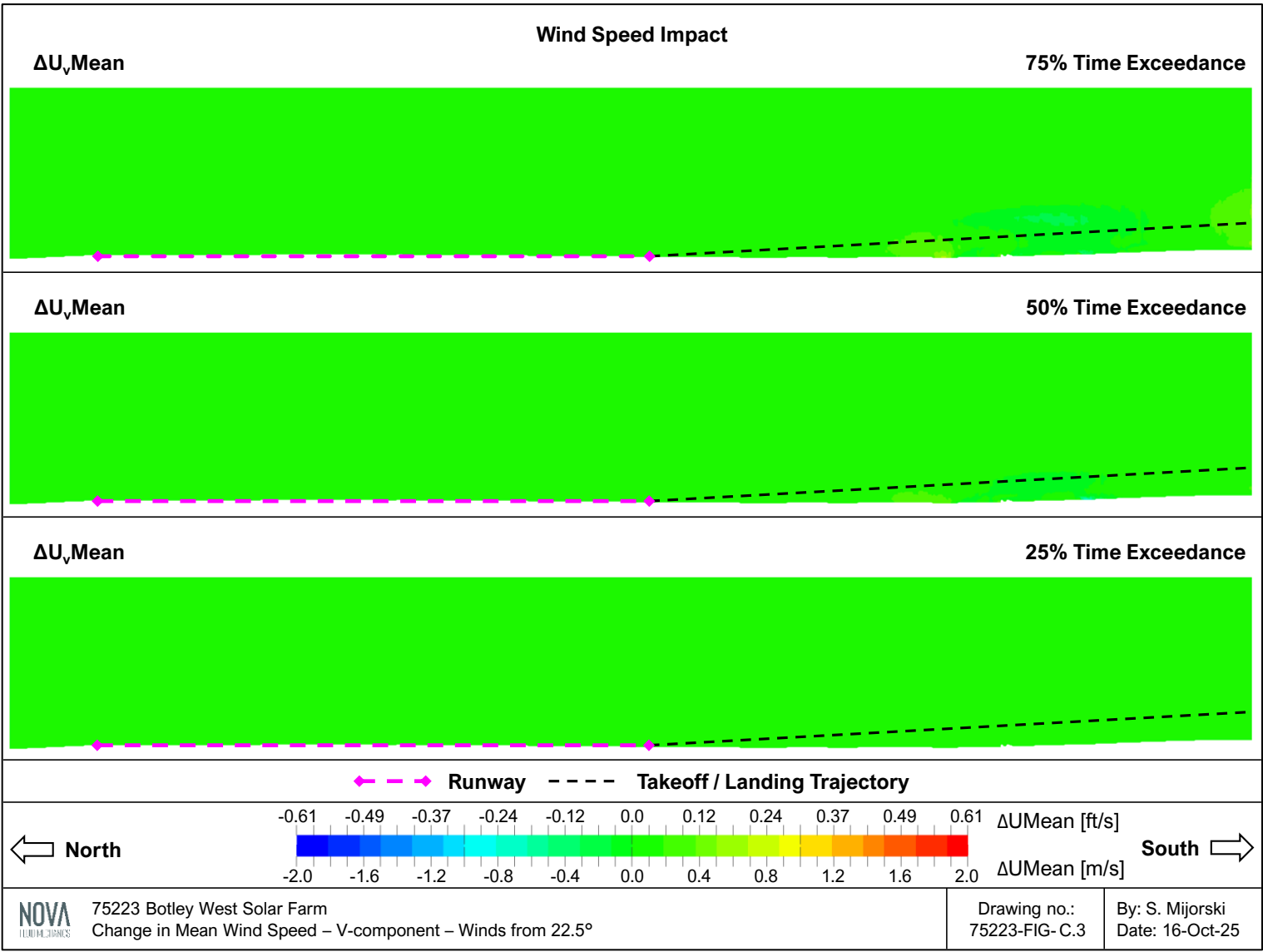


Figure C.4: Change in Mean Wind Speed – W-component – Winds from 22.5°

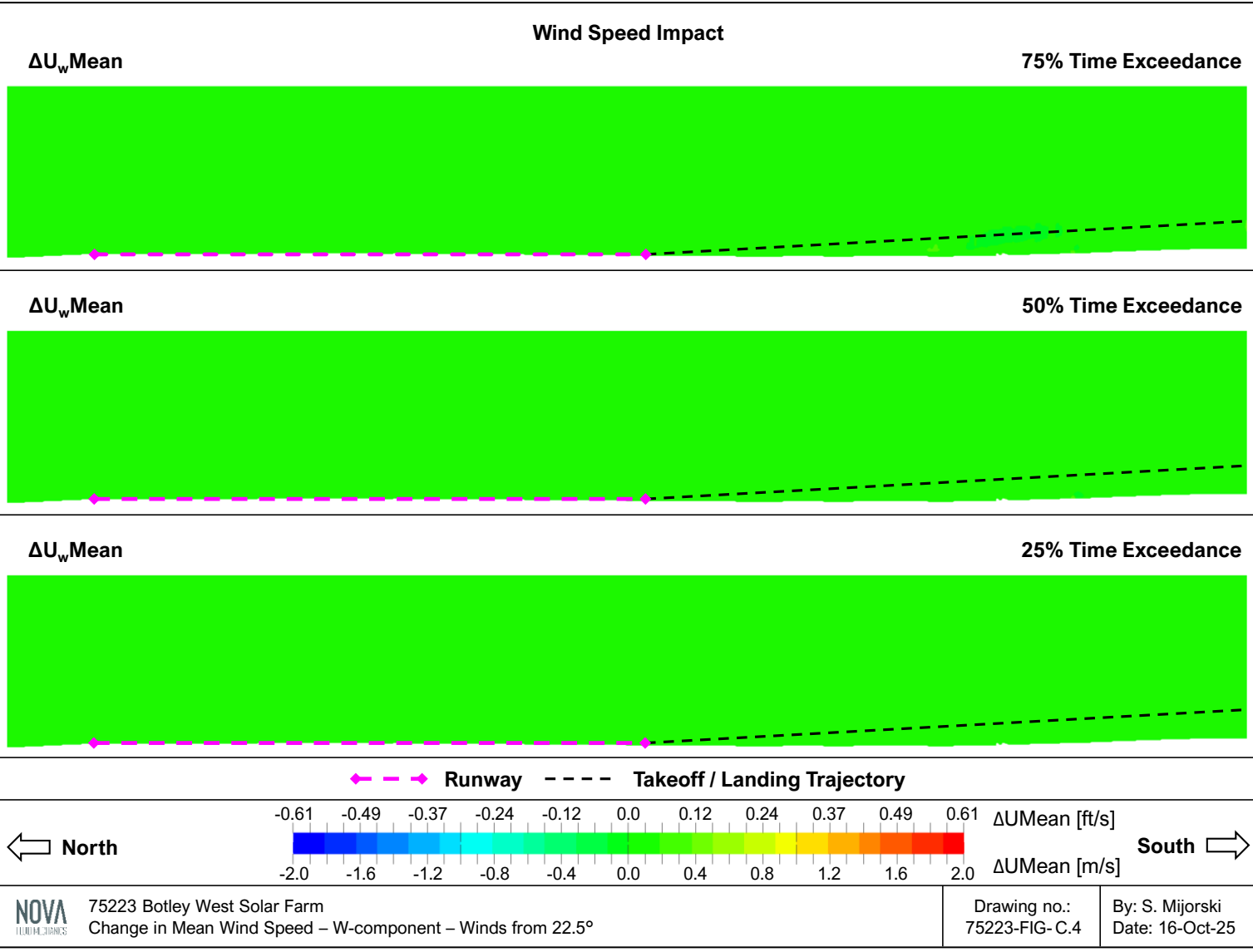


Figure C.5: Change in Air Temperature – Winds from 202.5°

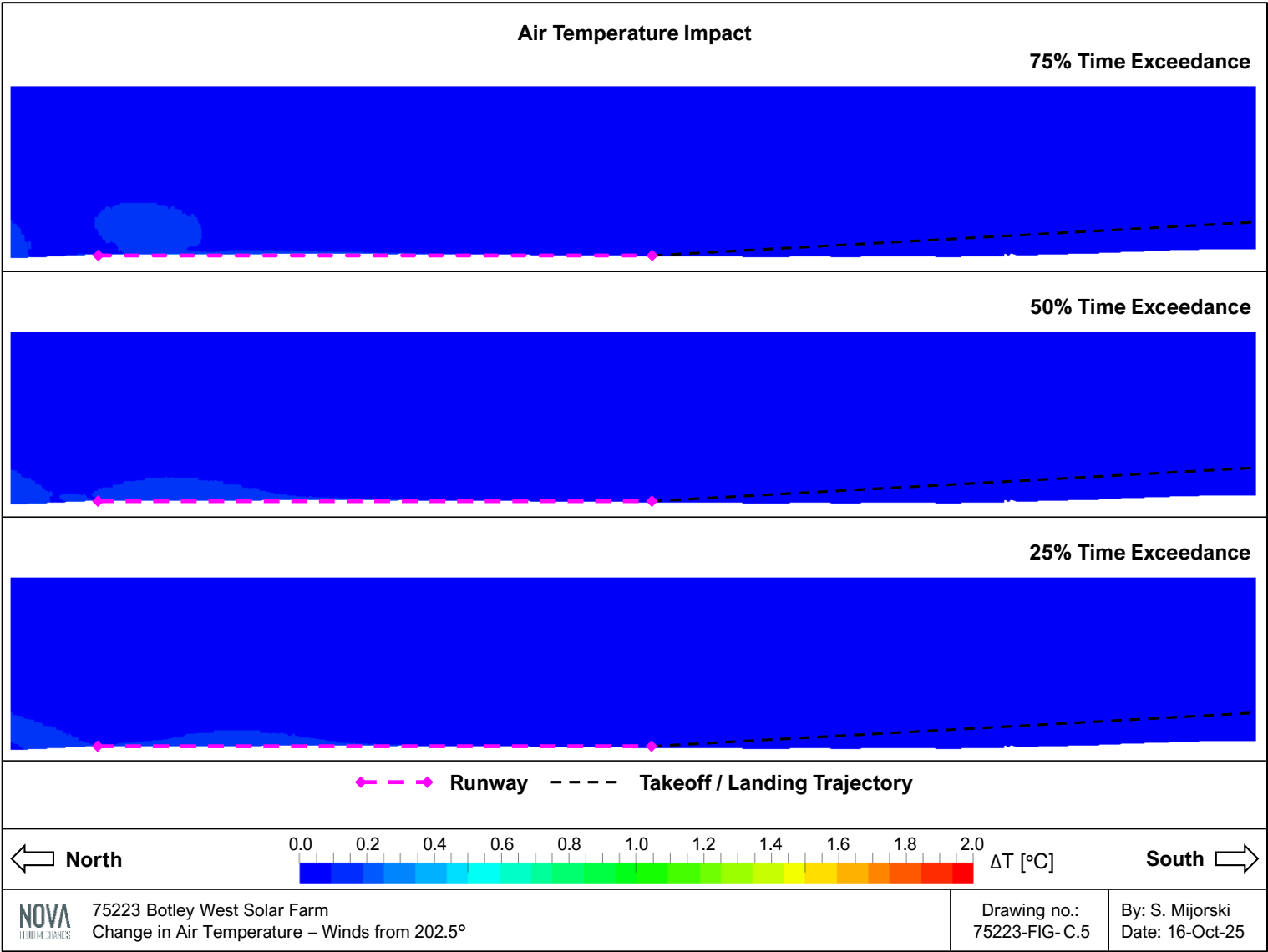


Figure C.6: Change in Mean Wind Speed – U-component – Winds from 202.5°

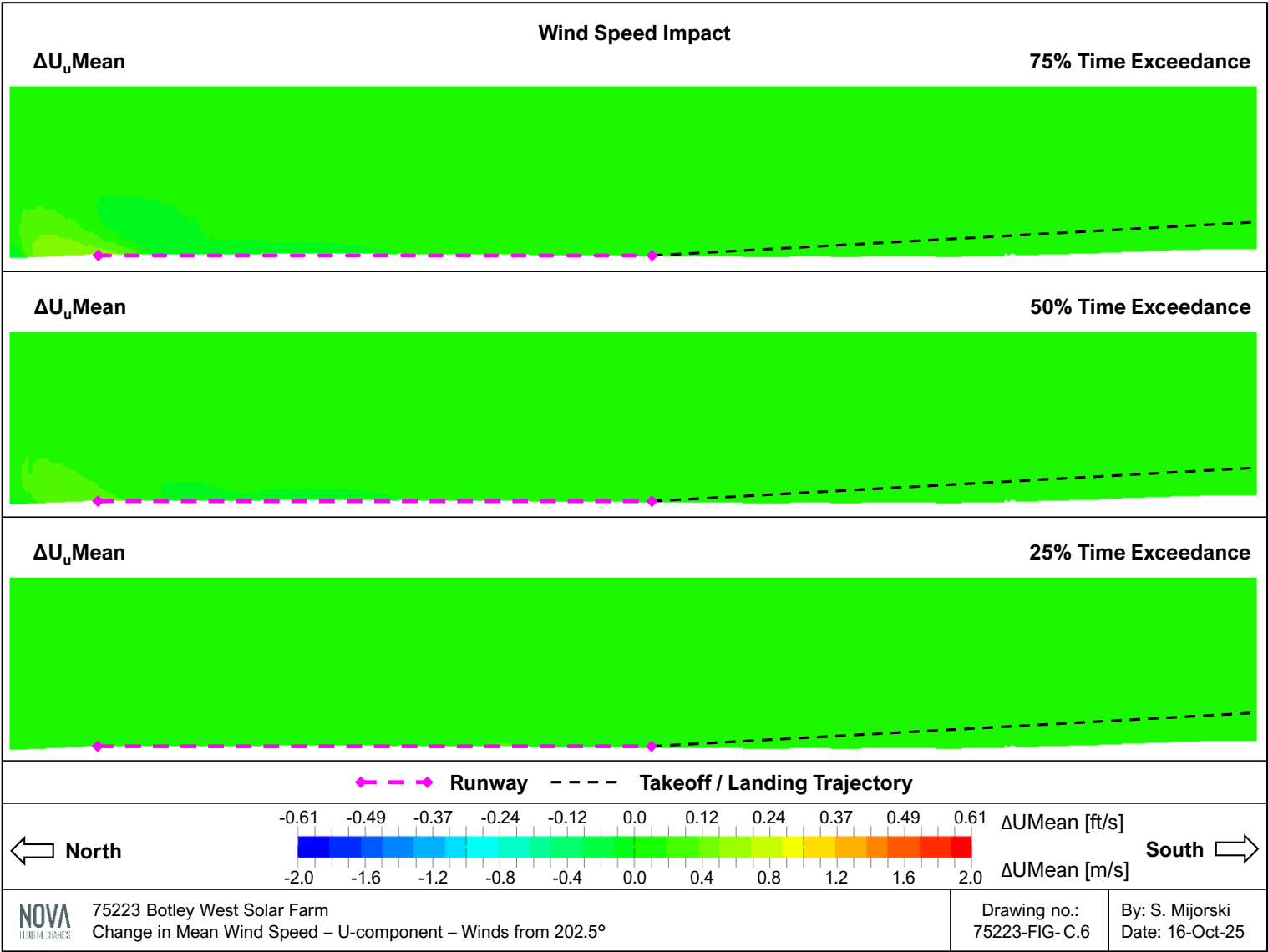


Figure C.7: Change in Mean Wind Speed – V-component – Winds from 202.5°

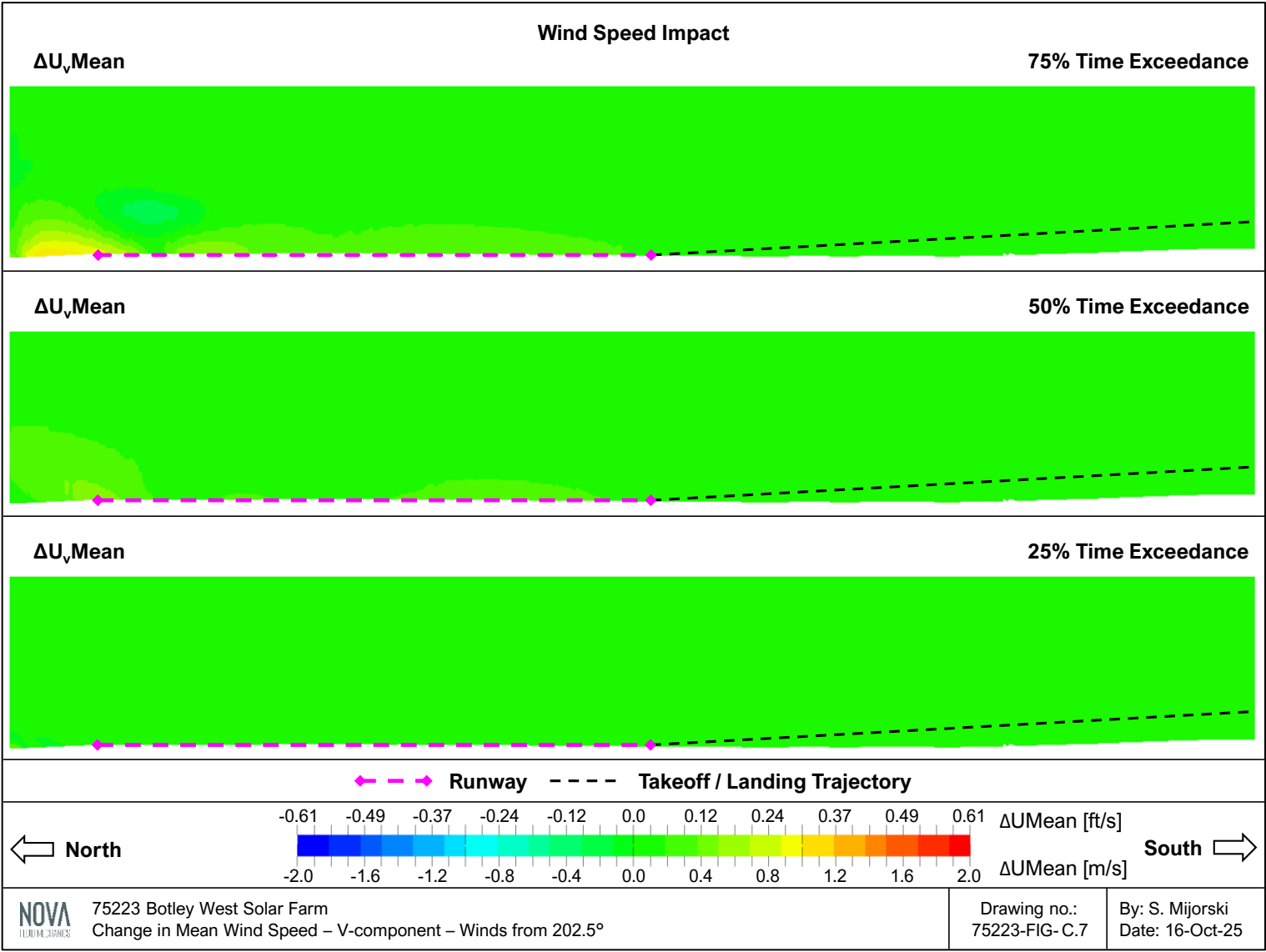


Figure C.8: Change in Mean Wind Speed – W-component – Winds from 202.5°

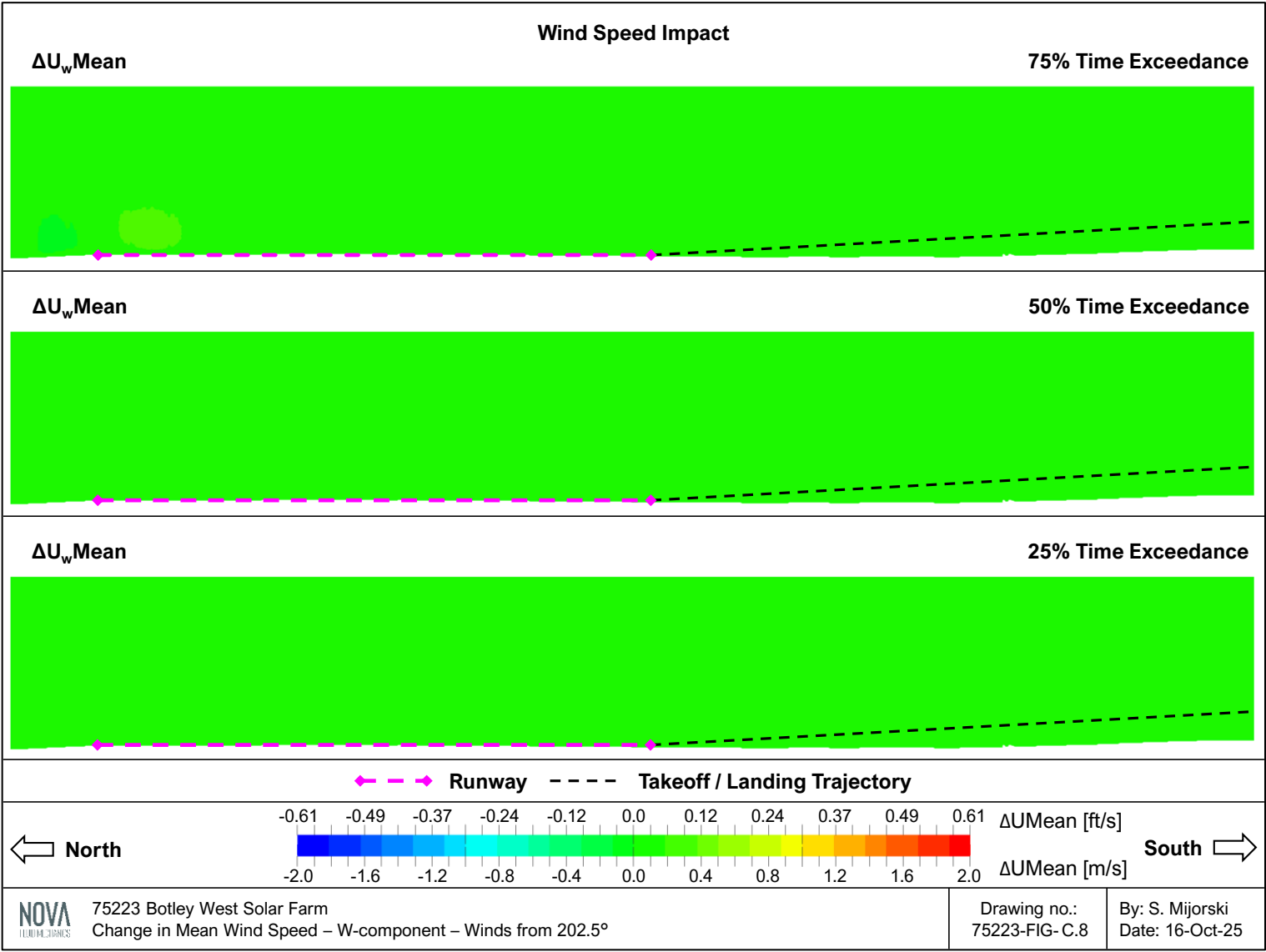


Figure C.9: Change in Air Temperature – Winds from 225.0°

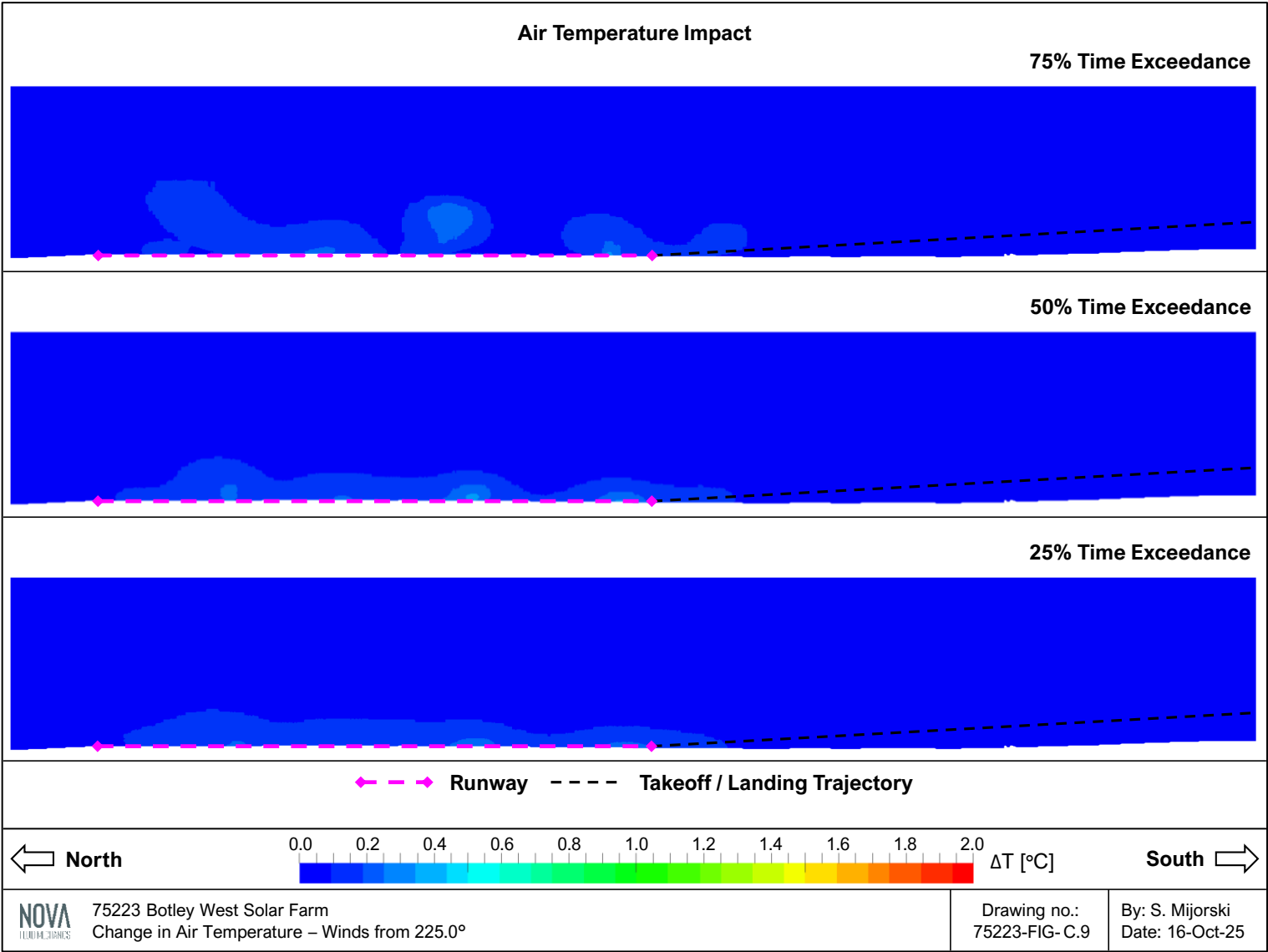


Figure C.10: Change in Mean Wind Speed – U-component – Winds from 225.0°

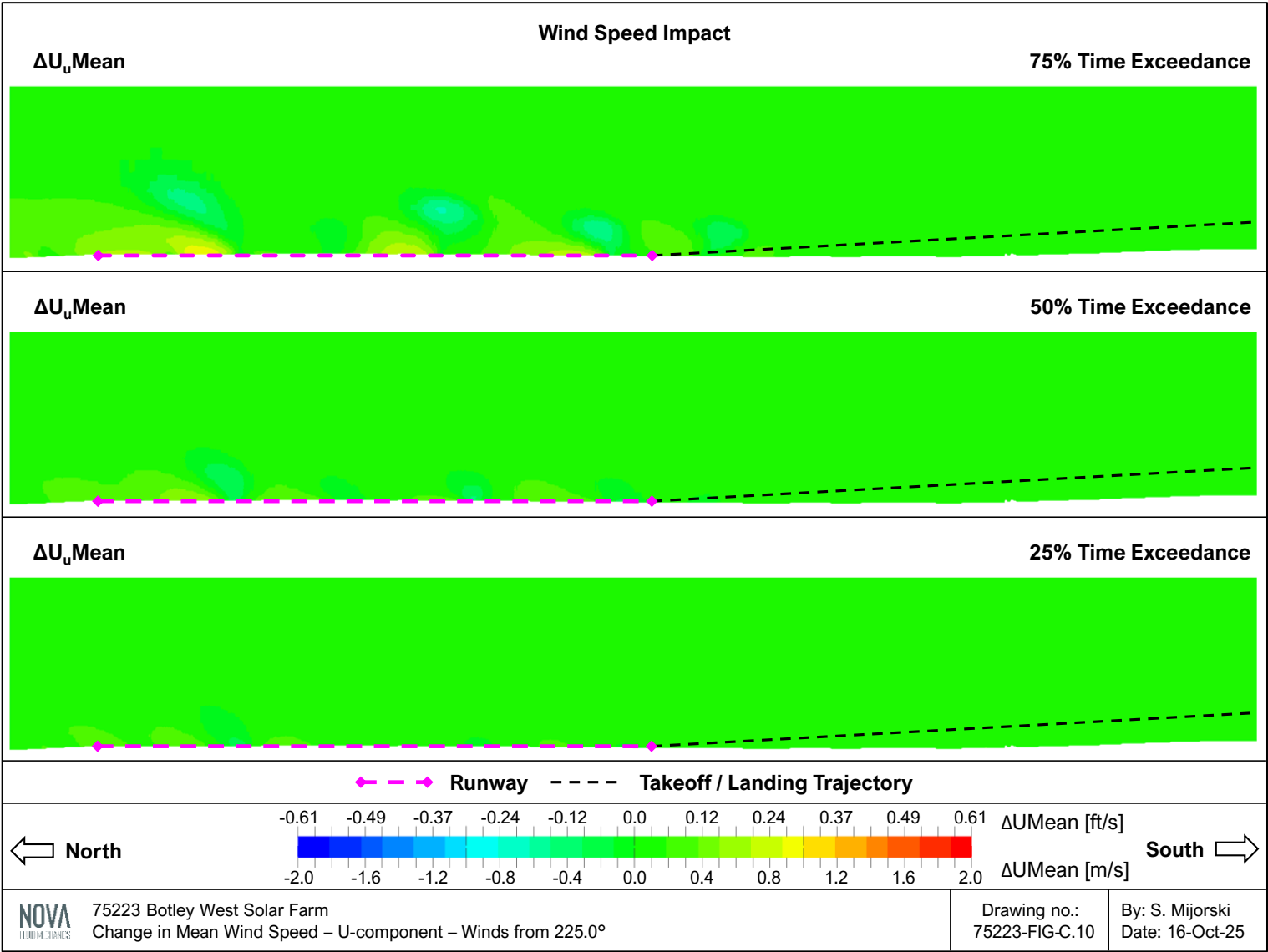


Figure C.11: Change in Mean Wind Speed – V-component – Winds from 225.0°

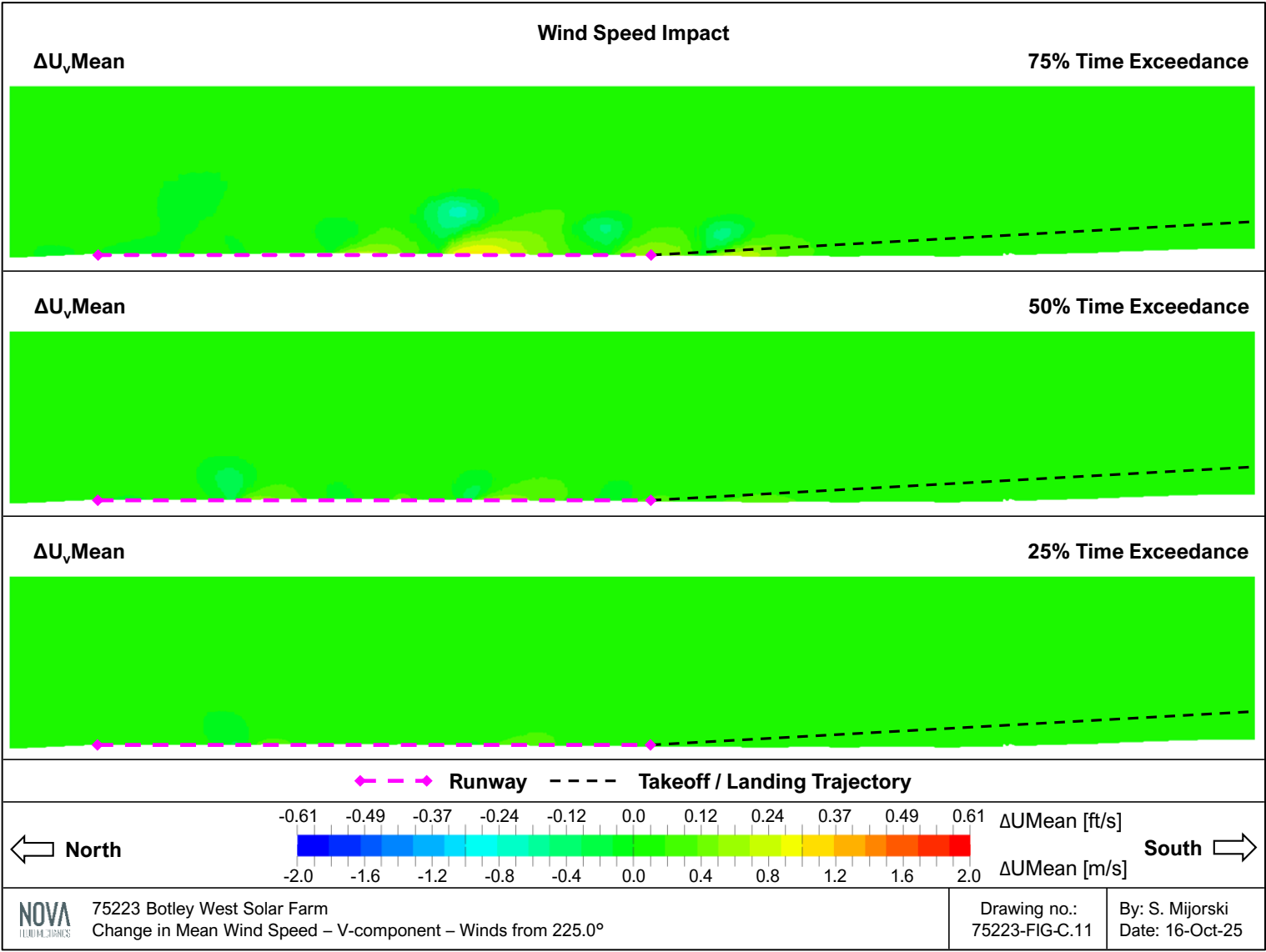


Figure C.12: Change in Mean Wind Speed – W-component – Winds from 225.0°

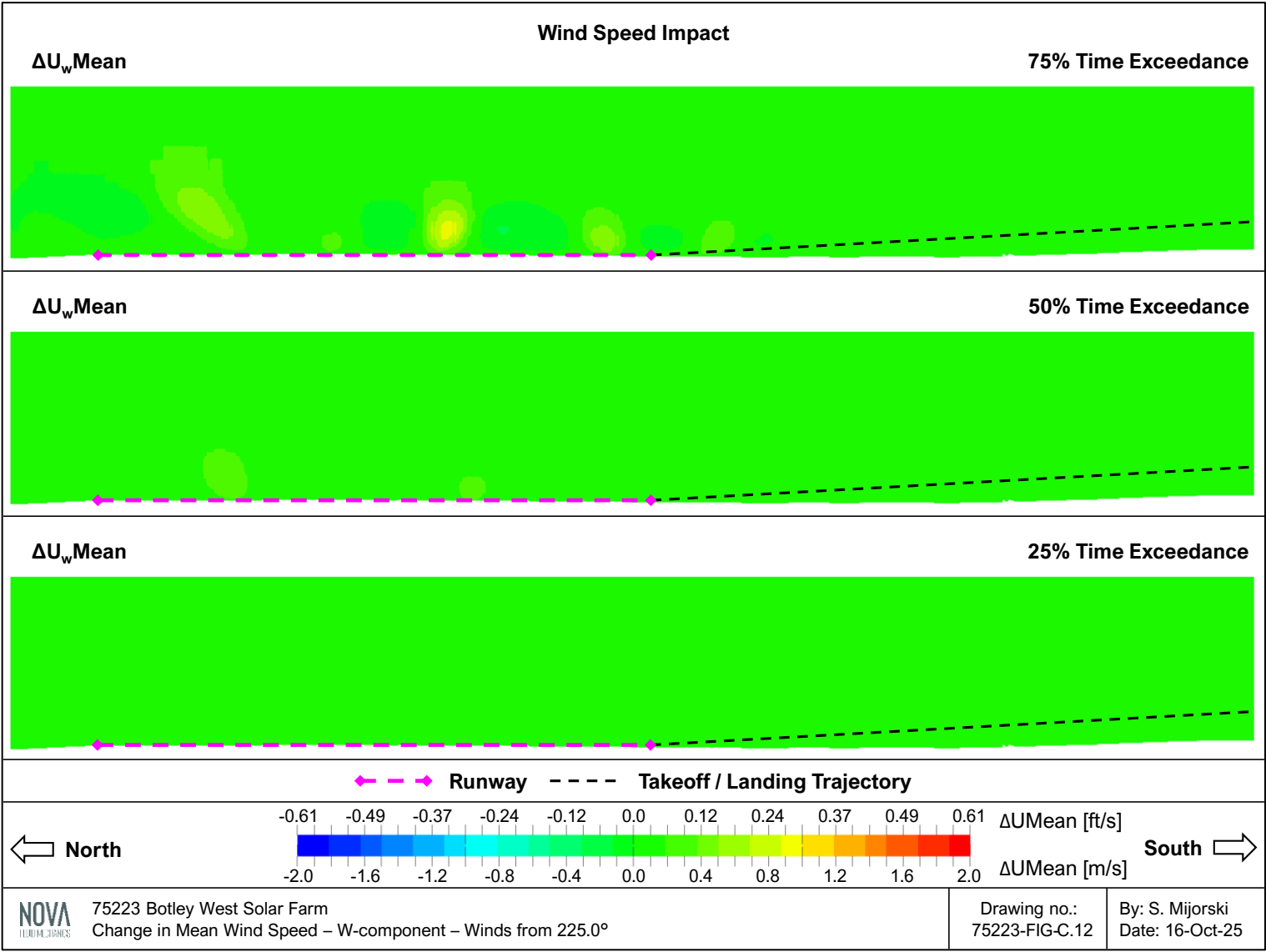


Figure C.13: Change in Air Temperature – Winds from 247.5°

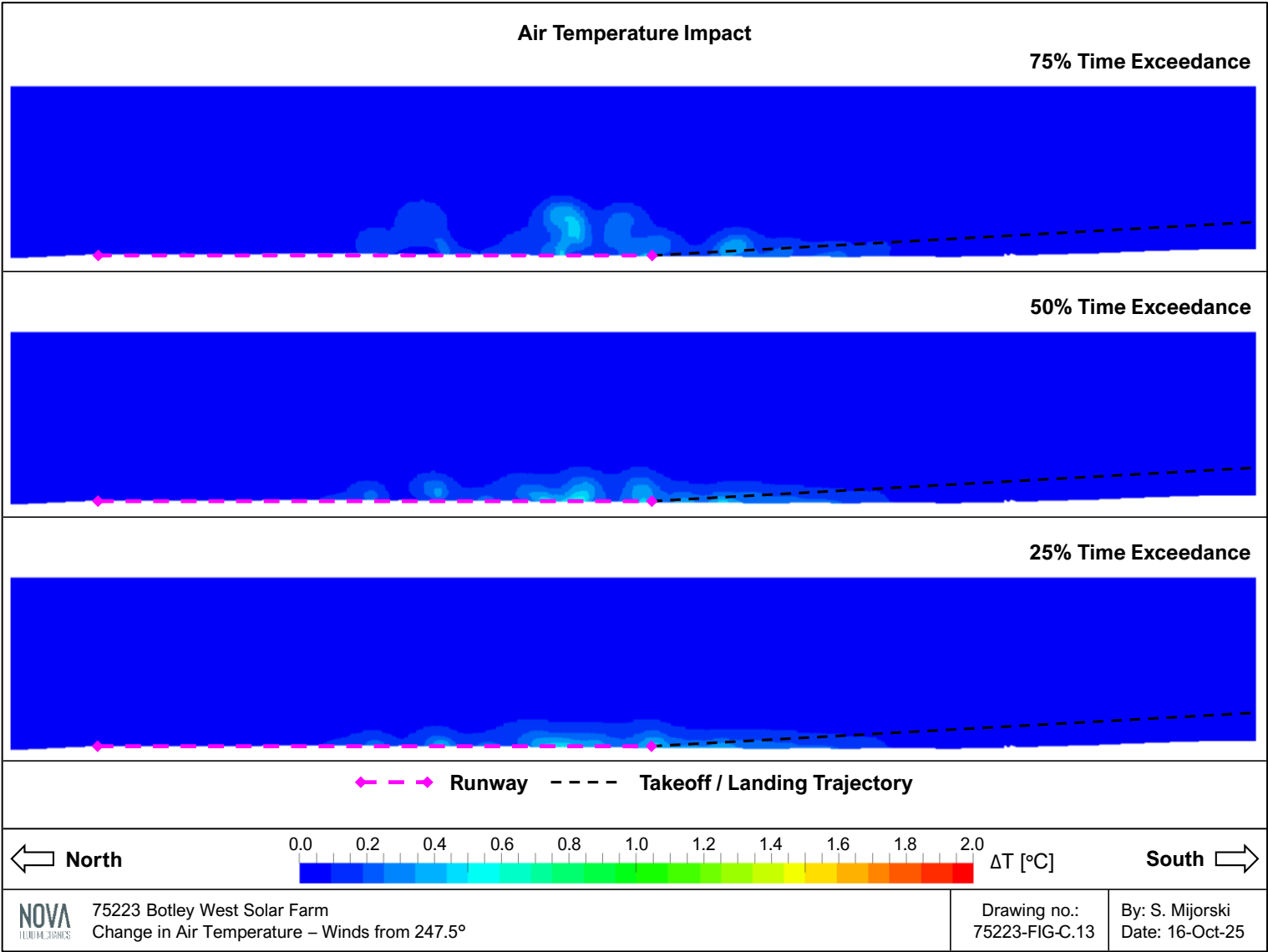


Figure C.14: Change in Mean Wind Speed – U-component – Winds from 247.5°

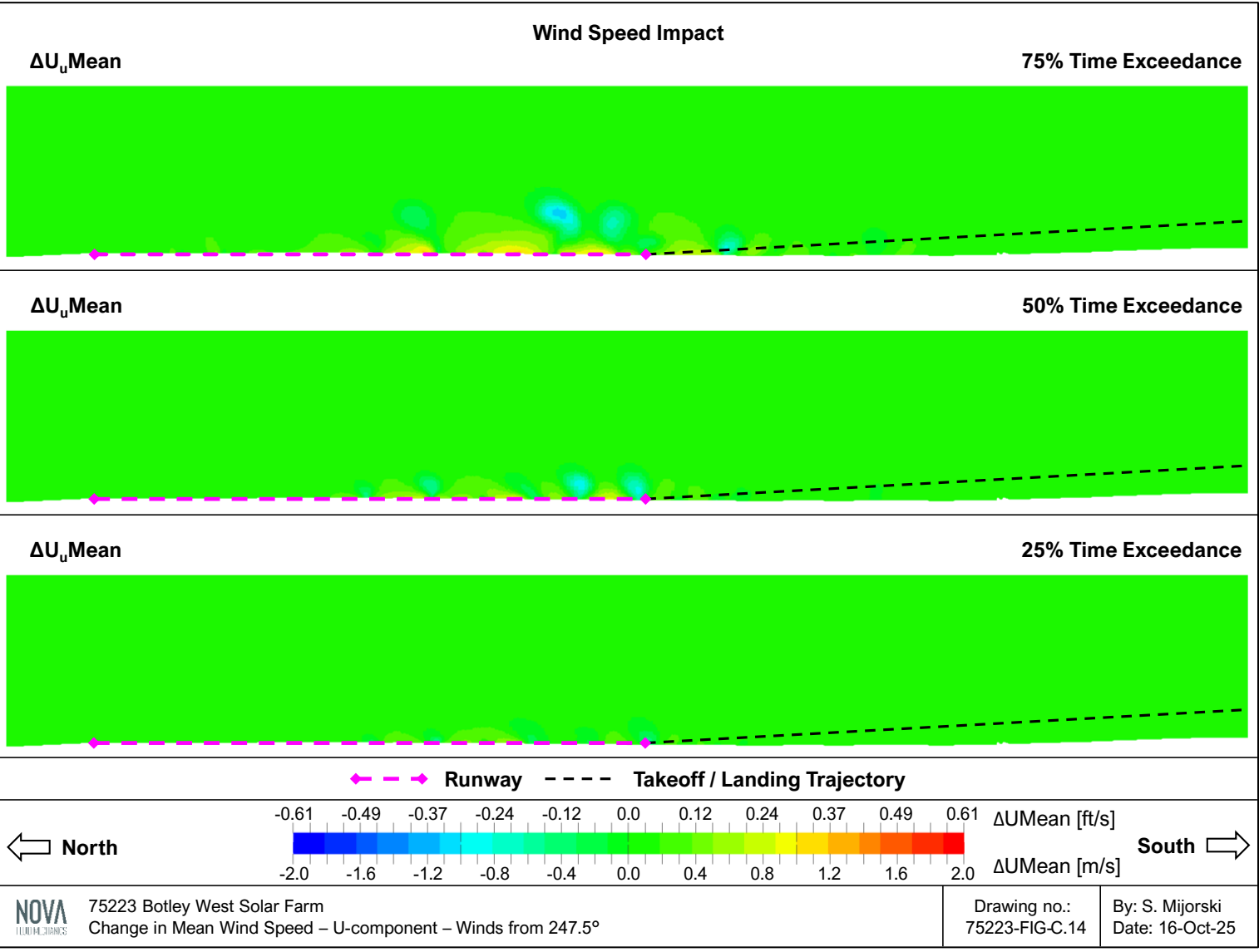


Figure C.15: Change in Mean Wind Speed – V-component – Winds from 247.5°

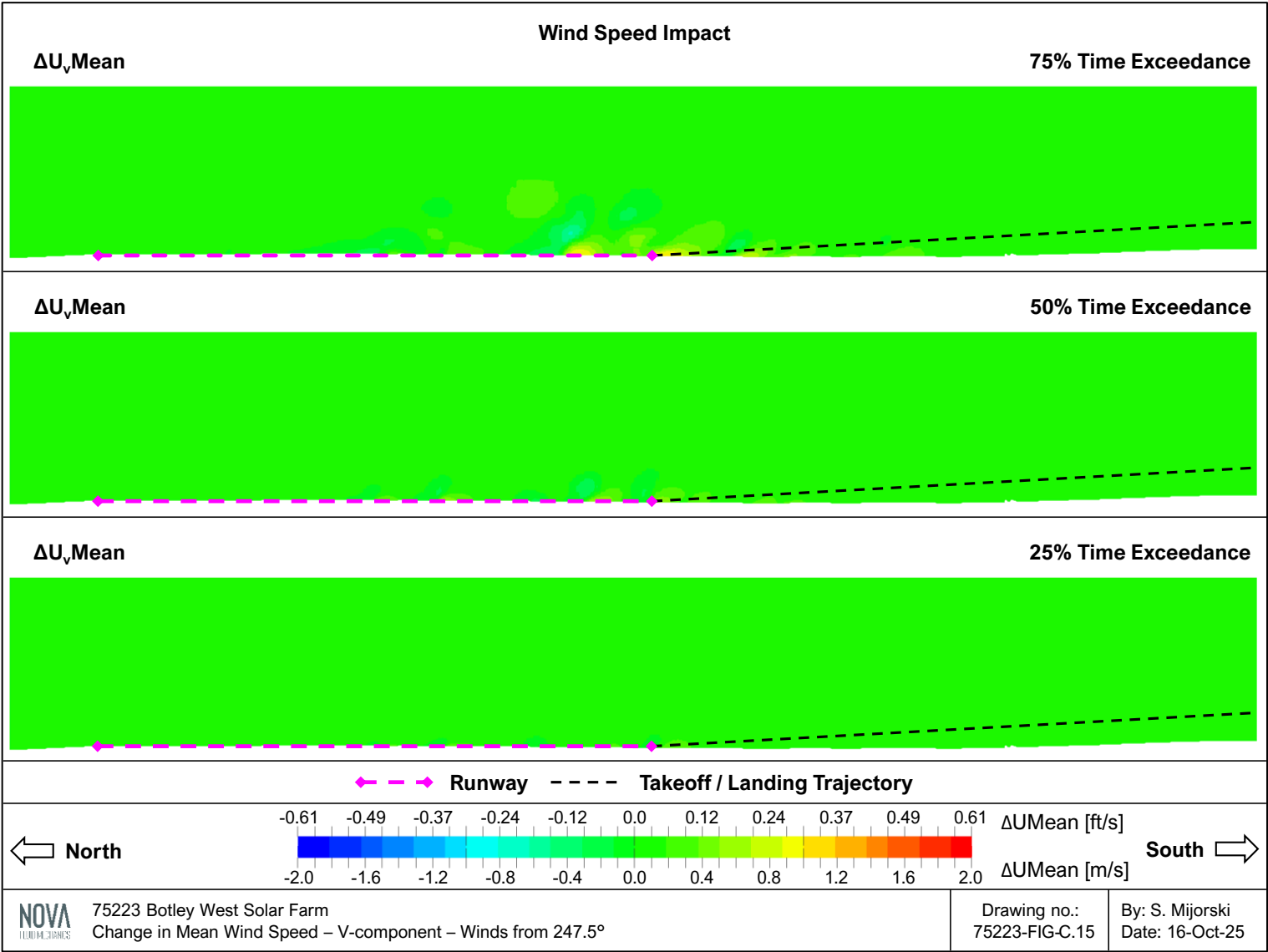


Figure C.16: Change in Mean Wind Speed – W-component – Winds from 247.5°

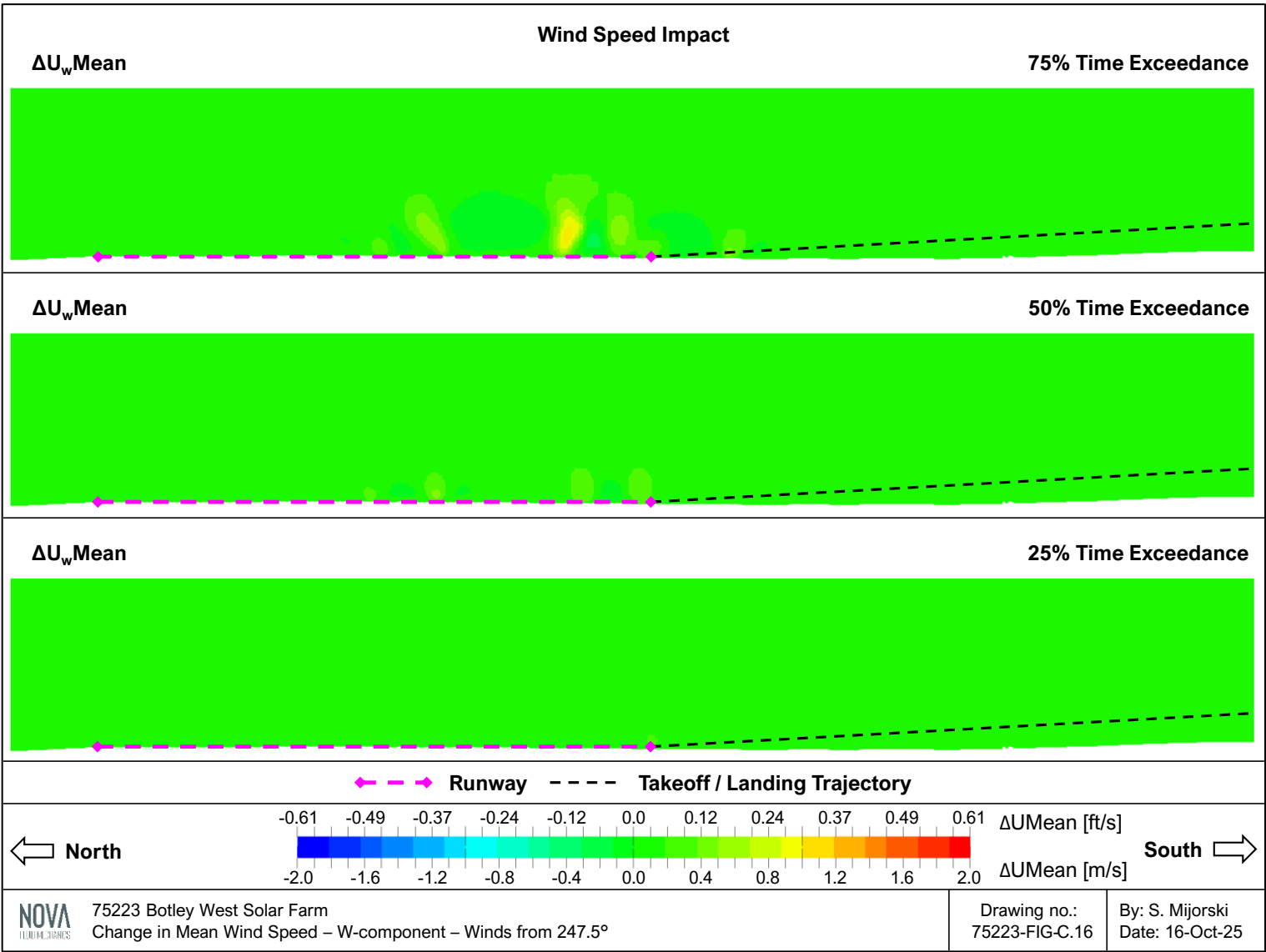


Figure C.17: Change in Air Temperature – Winds from 270.0°

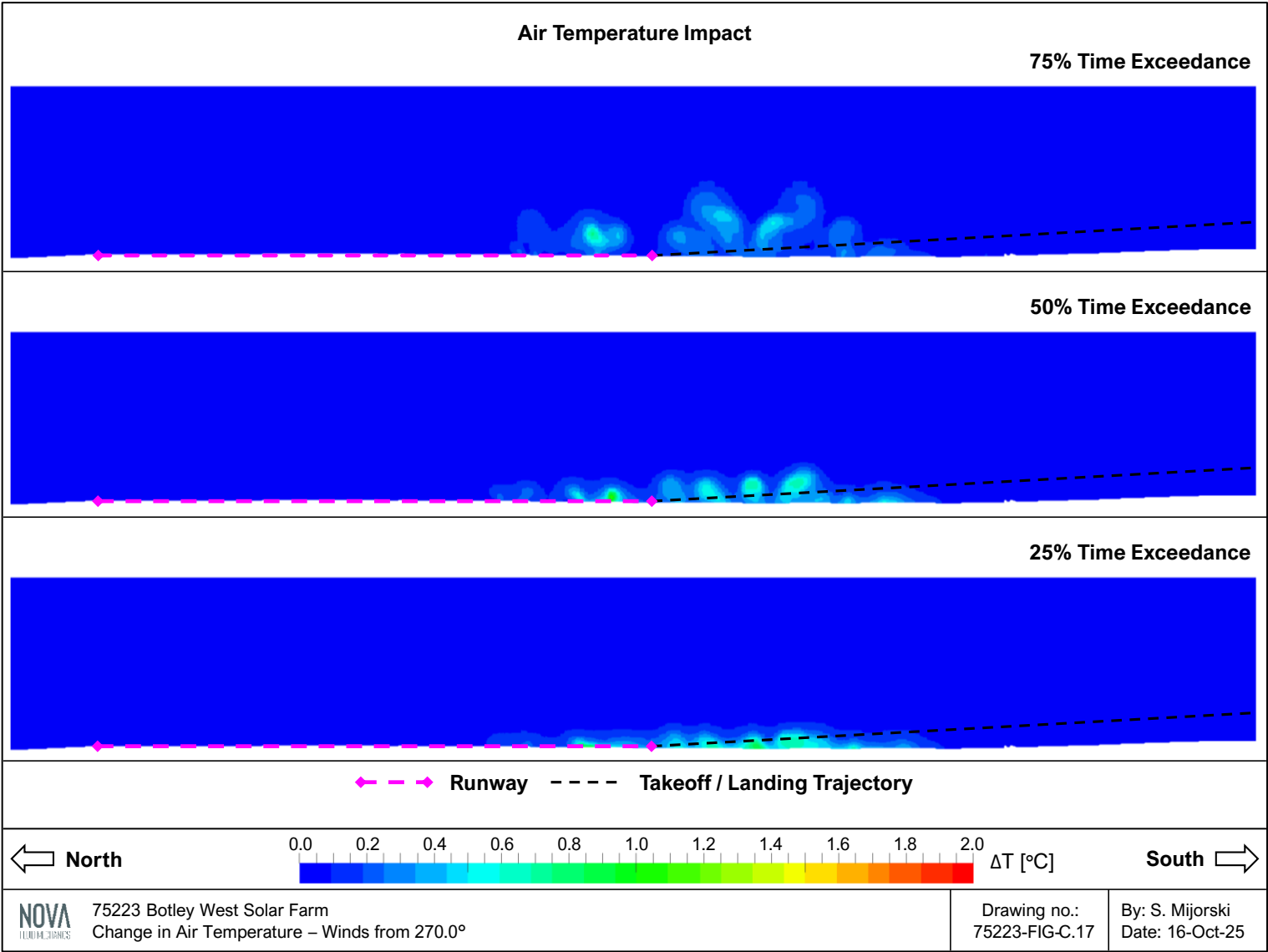


Figure C.18: Change in Mean Wind Speed – U-component – Winds from 270.0°

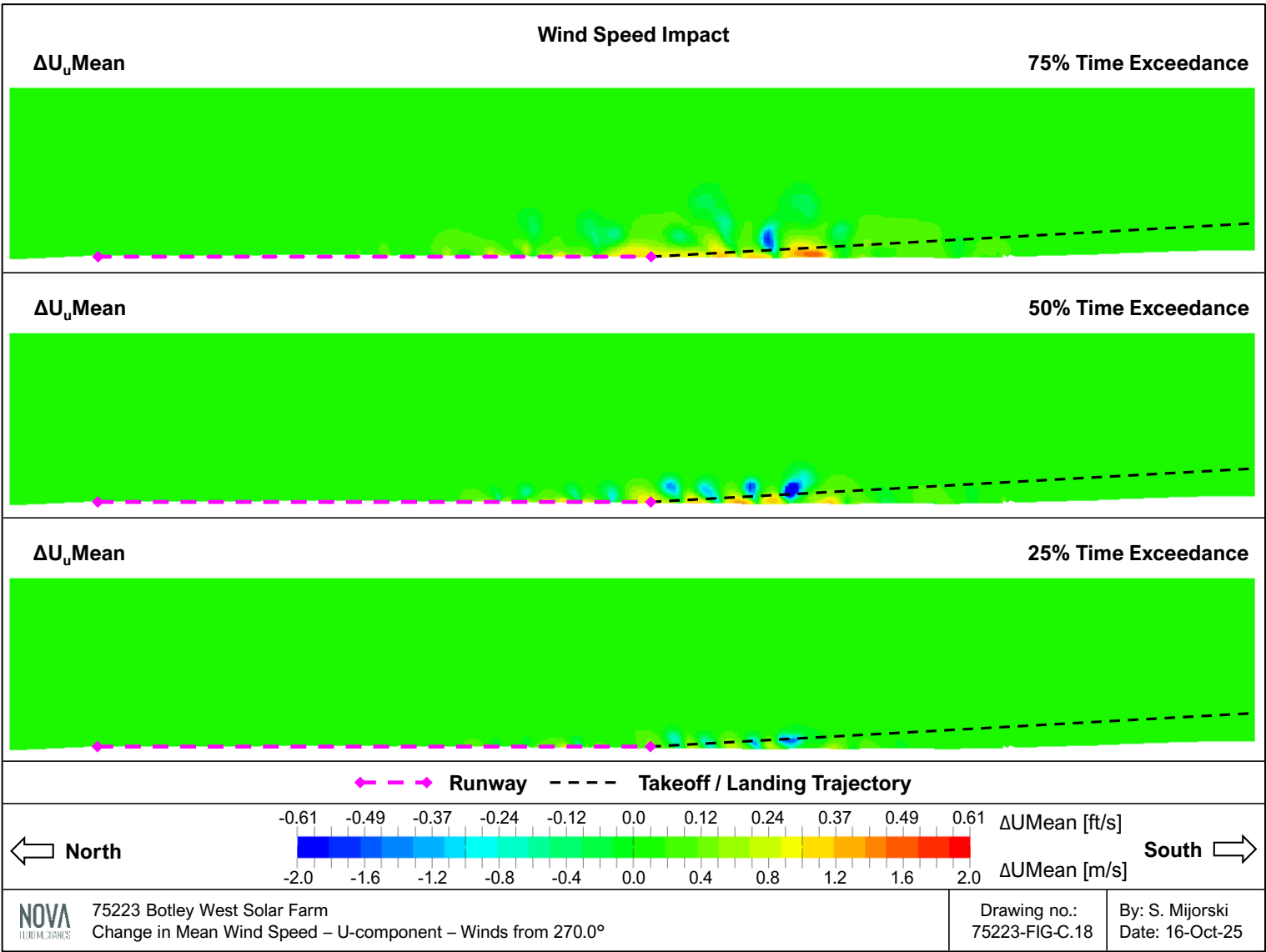


Figure C.19: Change in Mean Wind Speed – V-component – Winds from 270.0°

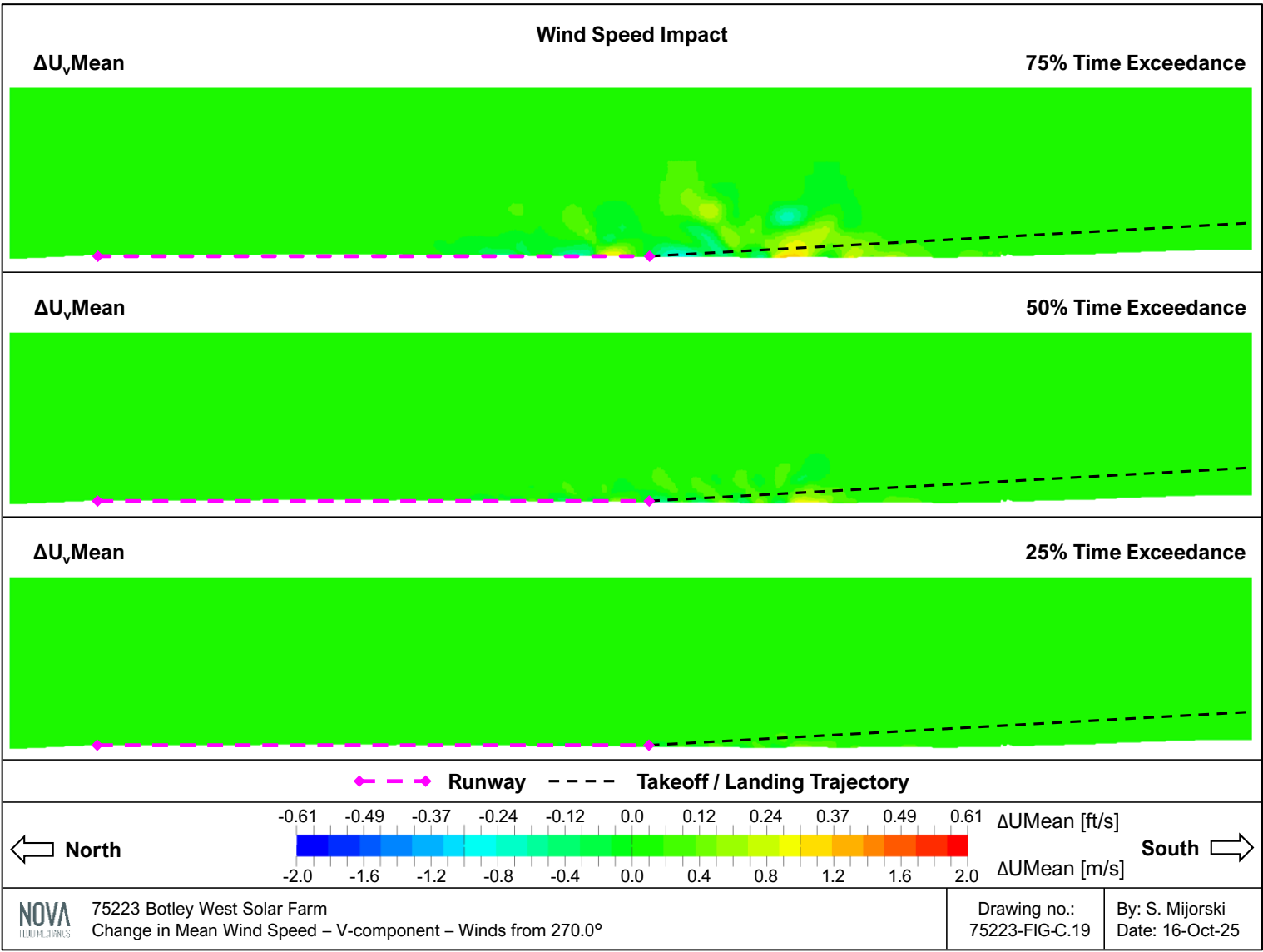


Figure C.20: Change in Mean Wind Speed – W-component – Winds from 270.0°

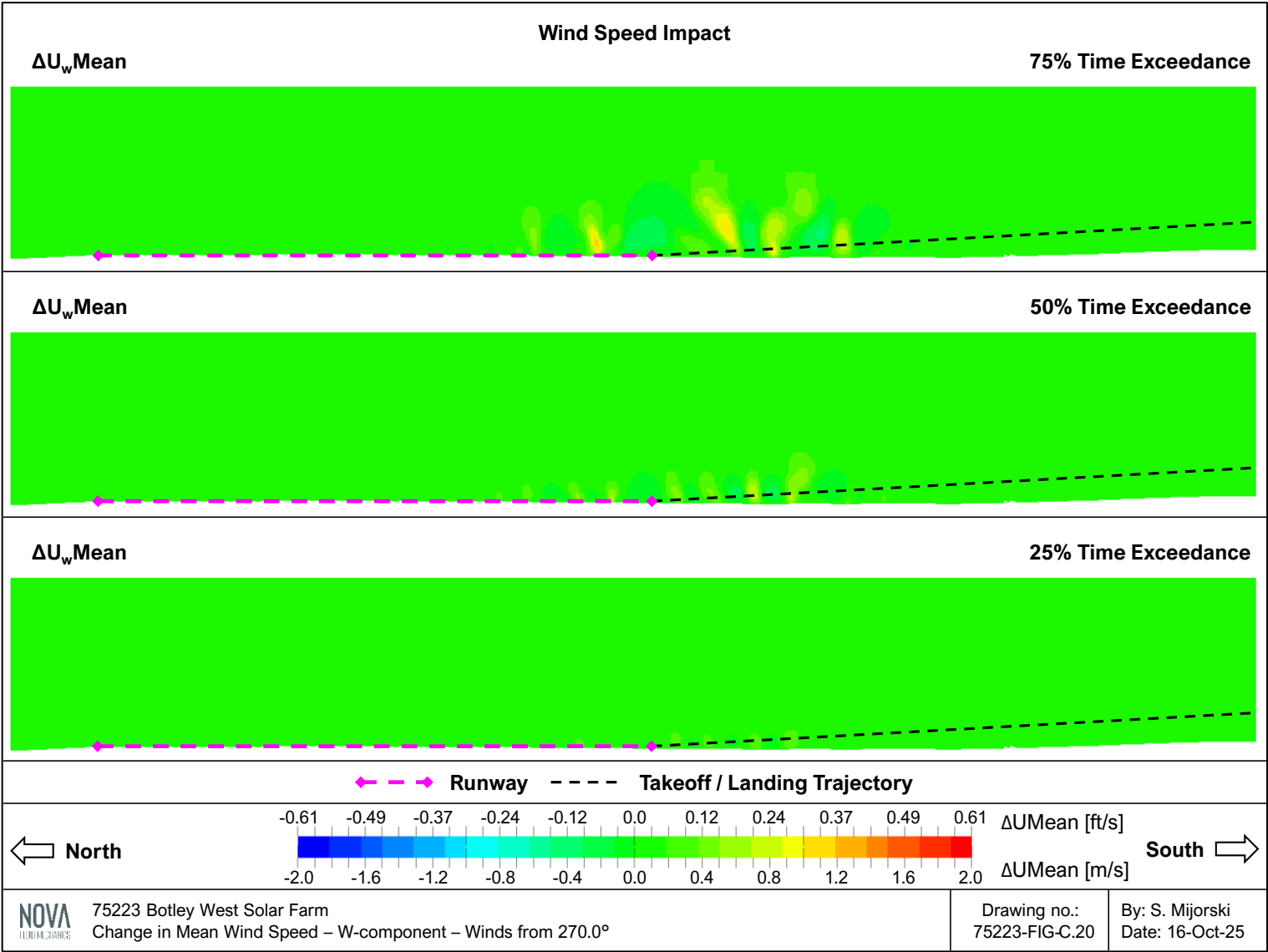


Figure C.21: Change in Air Temperature – Winds from 292.5°

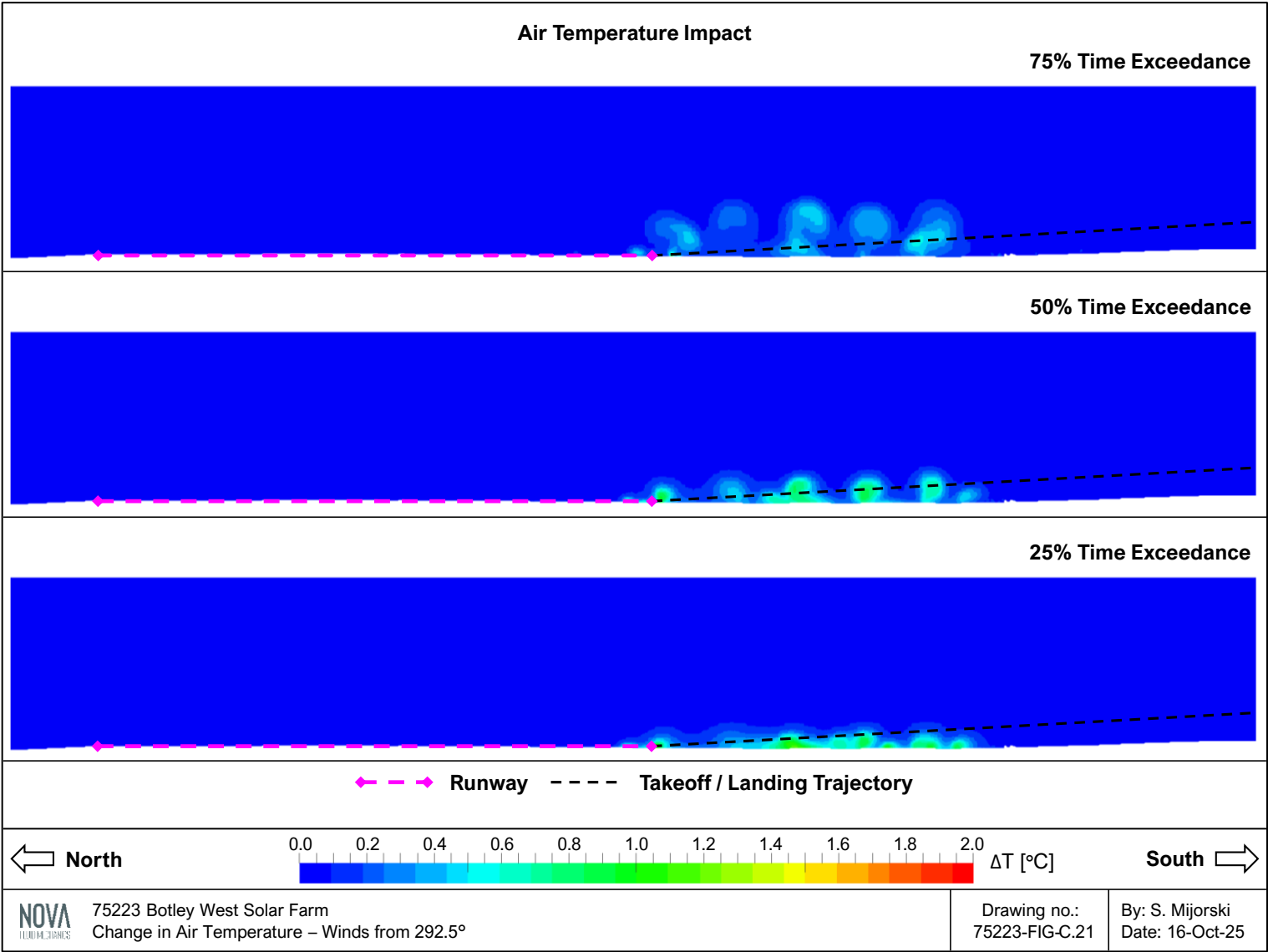


Figure C.22: Change in Mean Wind Speed – U-component – Winds from 292.5°

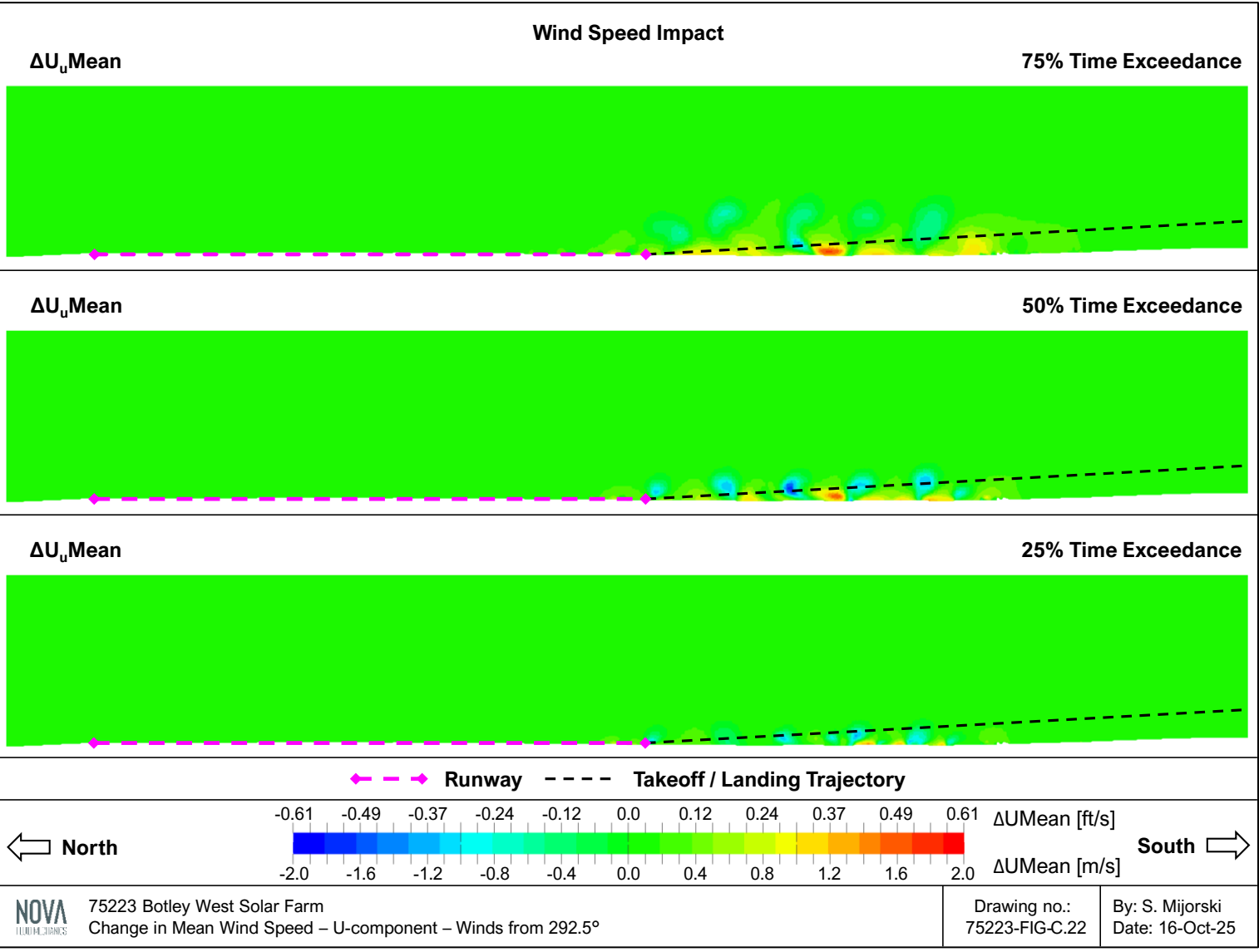


Figure C.23: Change in Mean Wind Speed – V-component – Winds from 292.5°

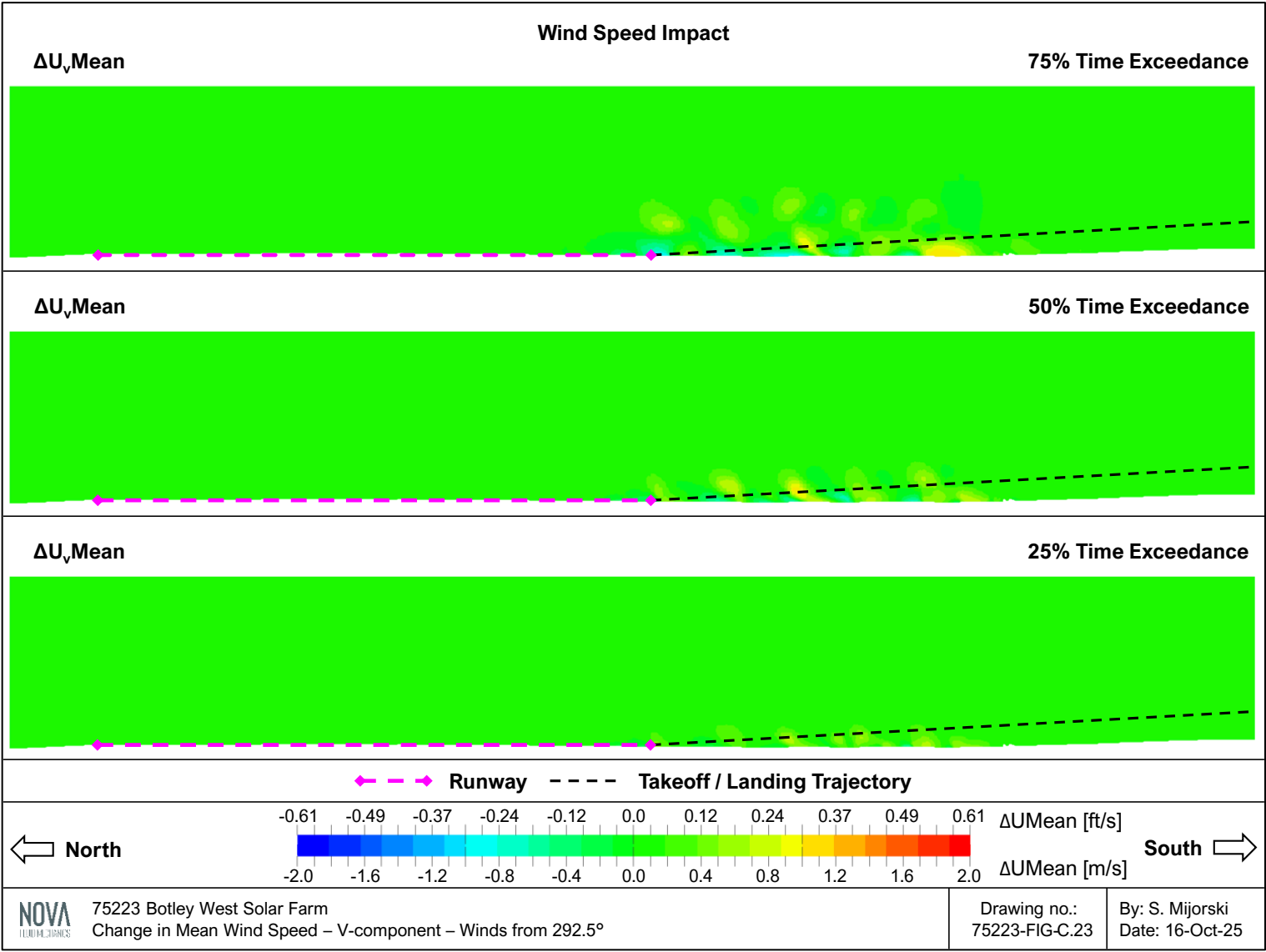


Figure C.24: Change in Mean Wind Speed – W-component – Winds from 292.5°

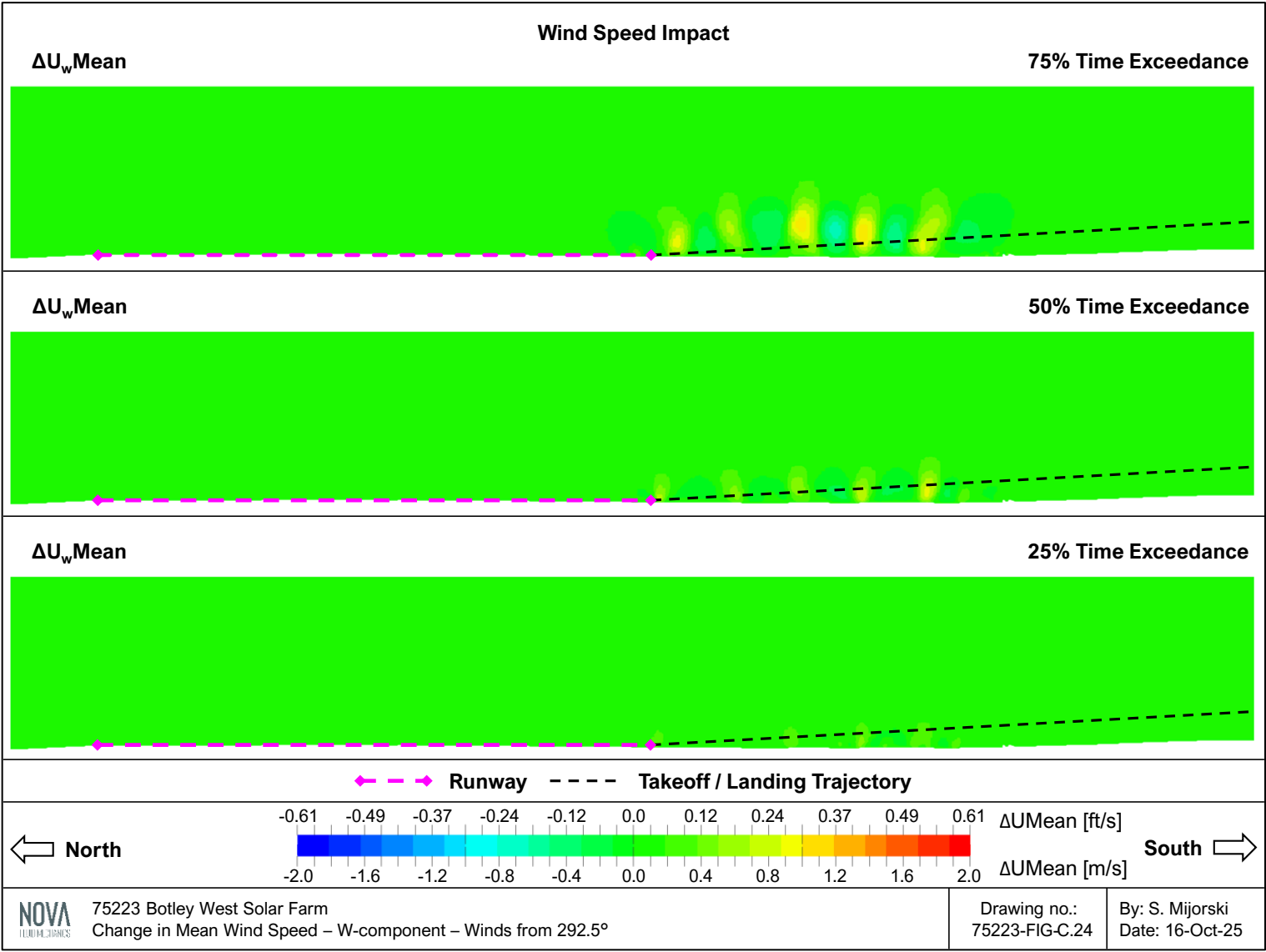


Figure C.25: Change in Air Temperature – Winds from 315.0°

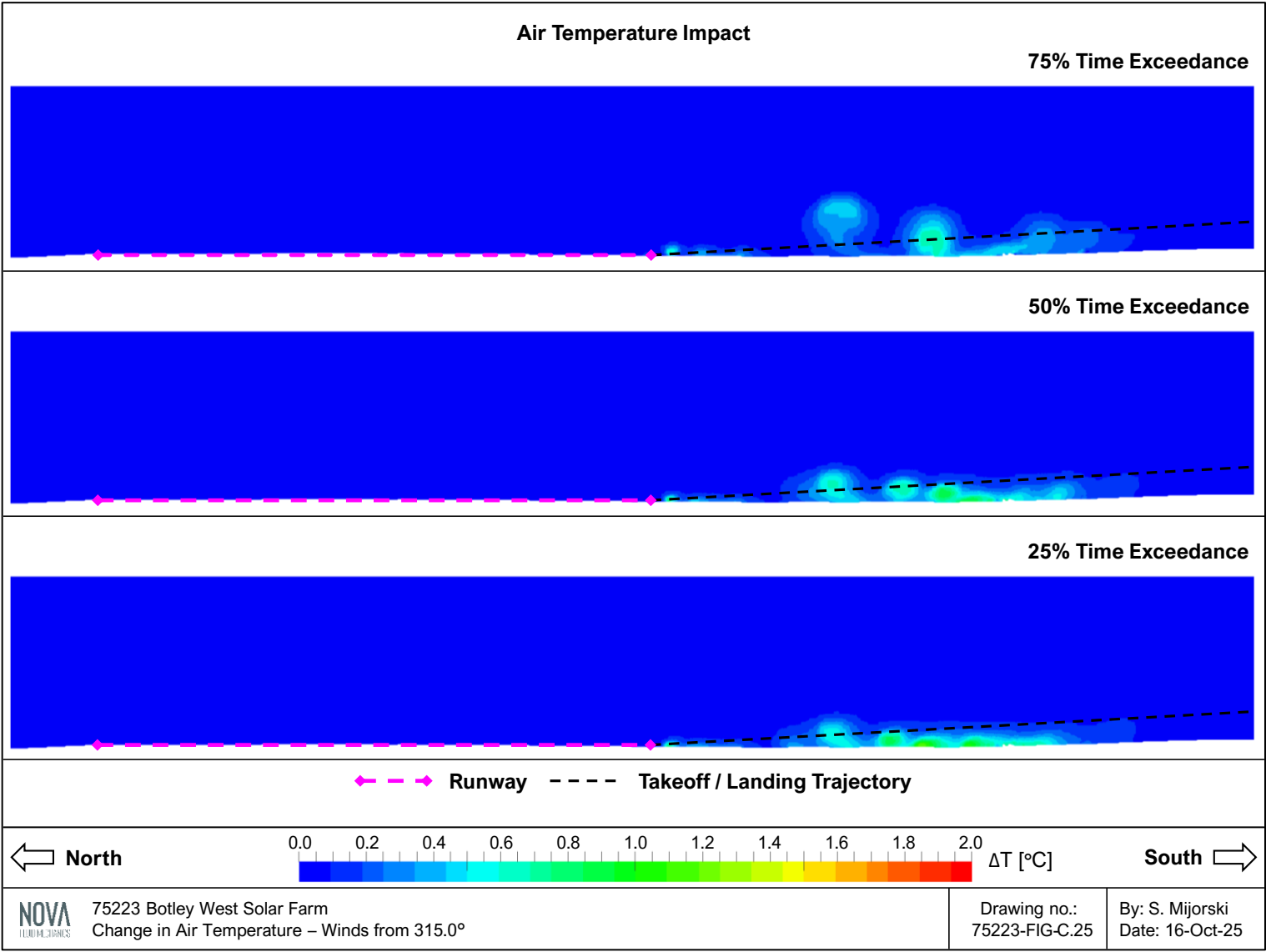


Figure C.26: Change in Mean Wind Speed – U-component – Winds from 315.0°

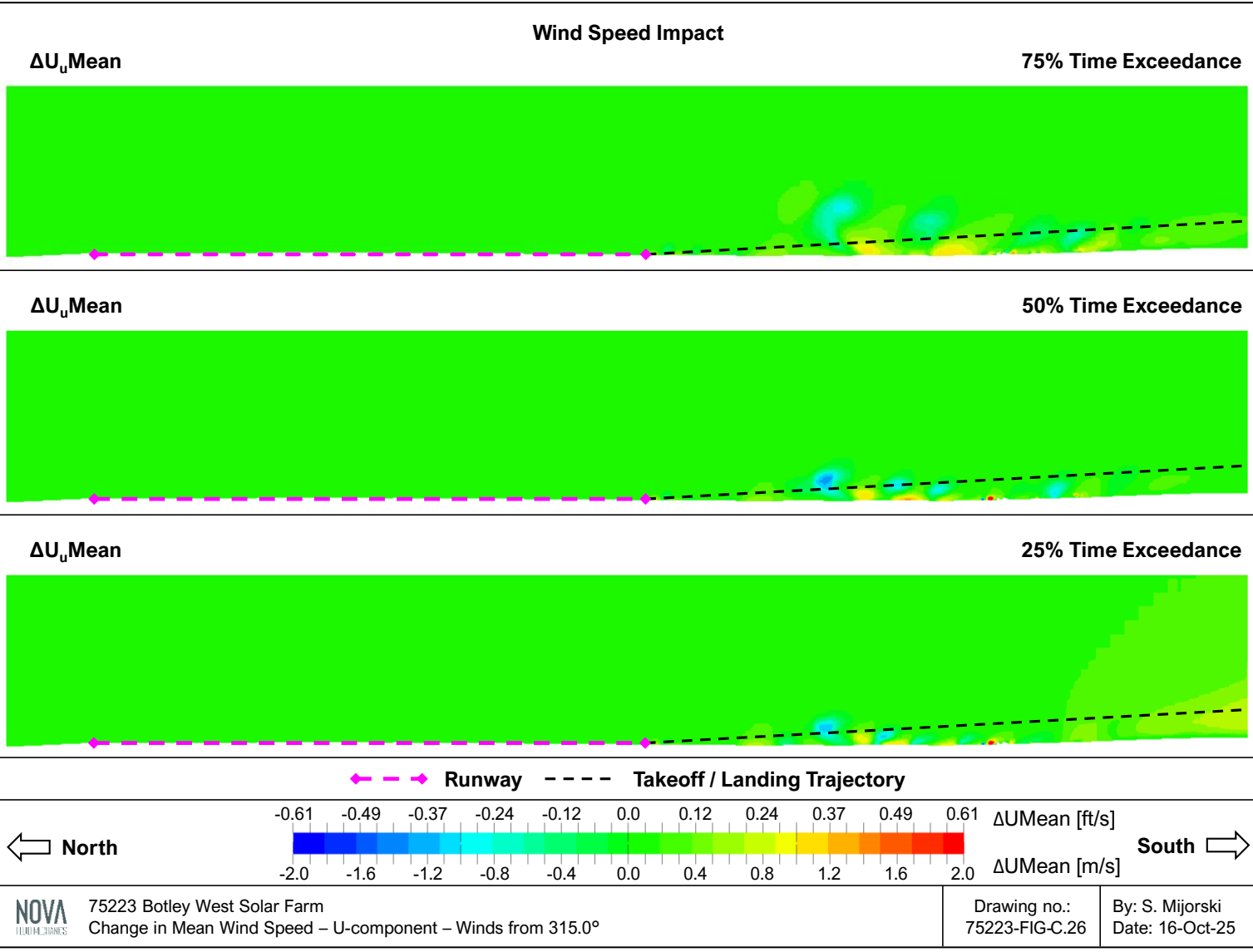


Figure C.27: Change in Mean Wind Speed – V-component – Winds from 315.0°

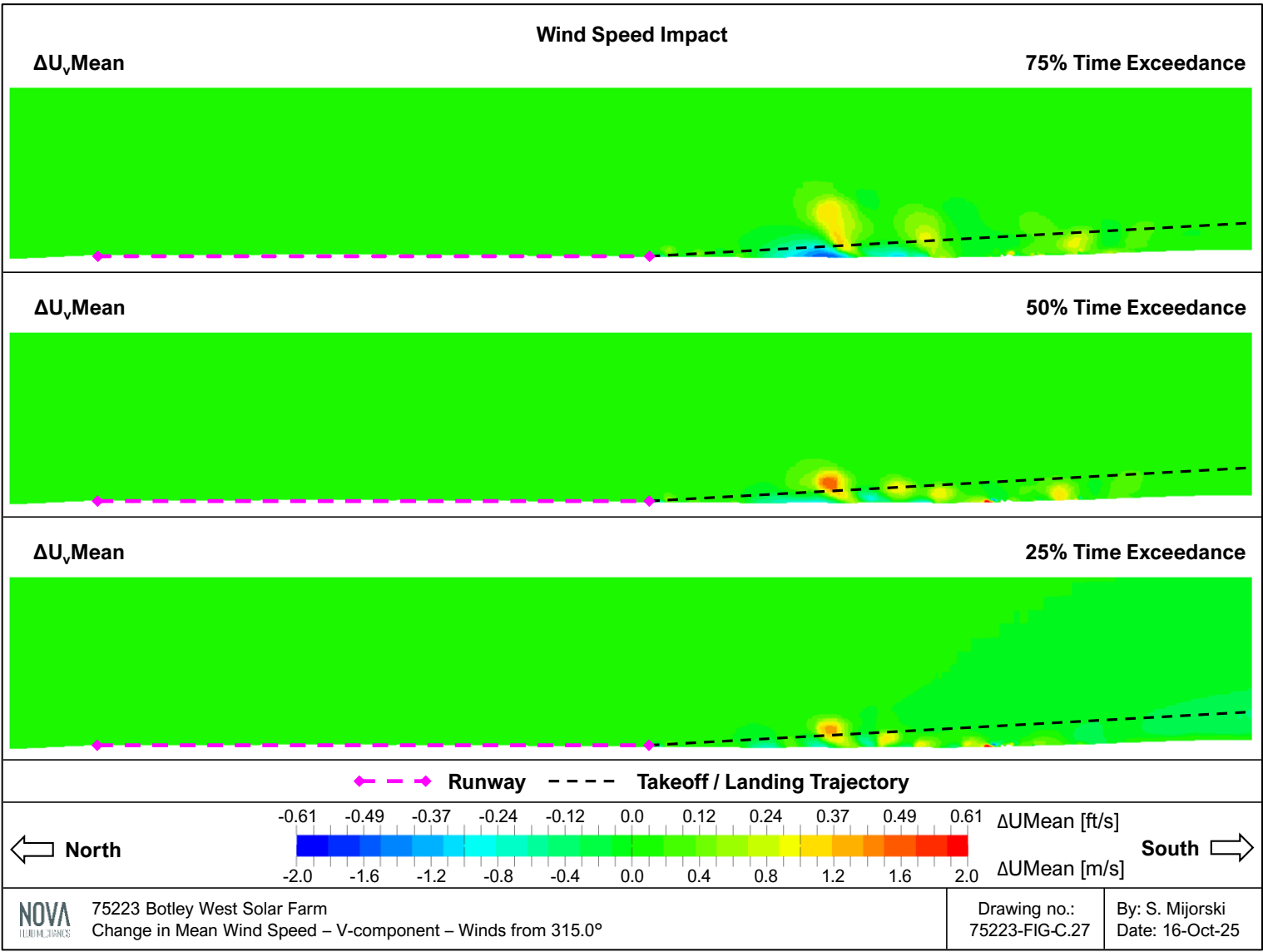


Figure C.28: Change in Mean Wind Speed – W-component – Winds from 315.0°

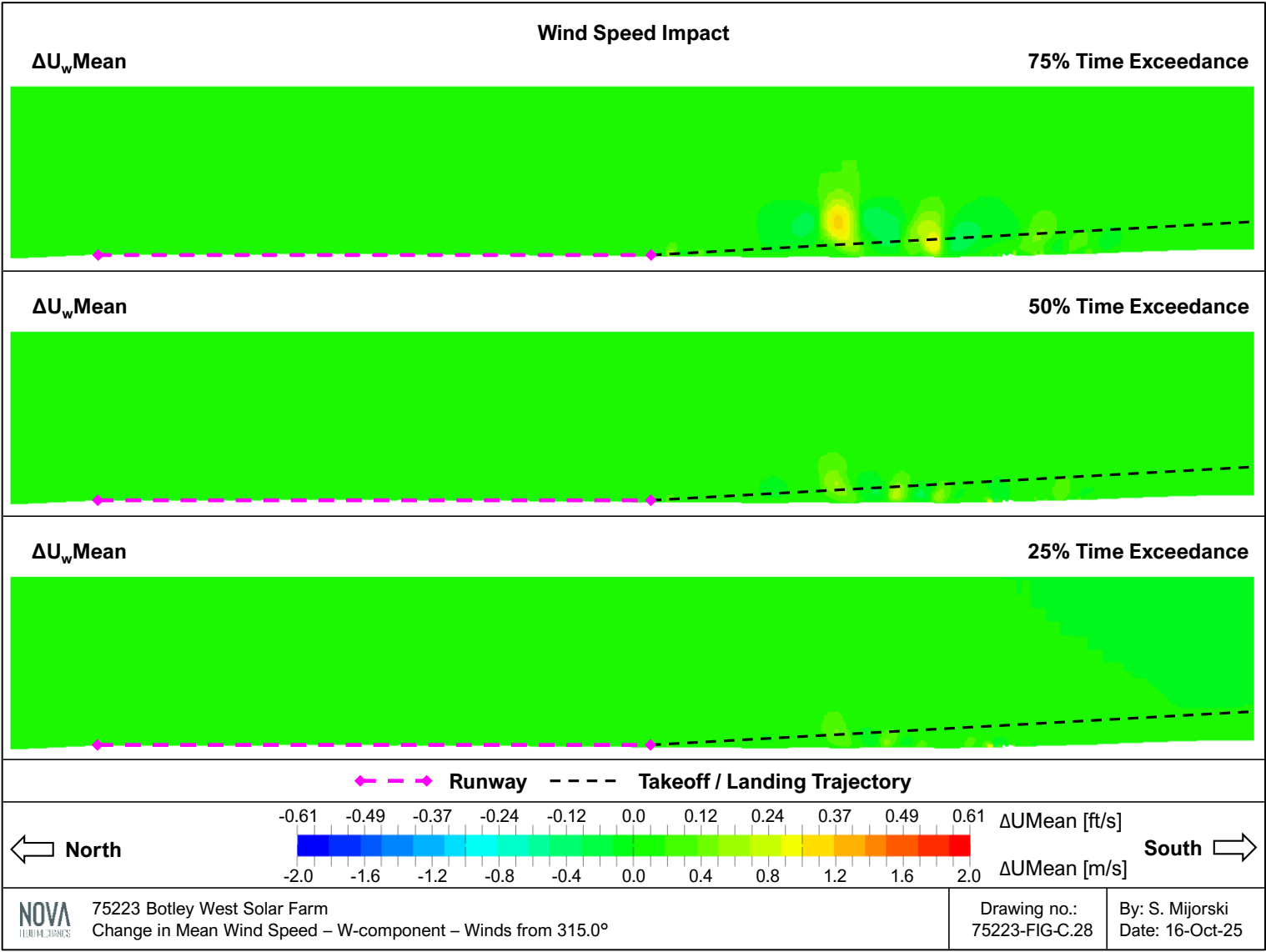


Figure C.29: Change in Air Temperature – Winds from 337.5°

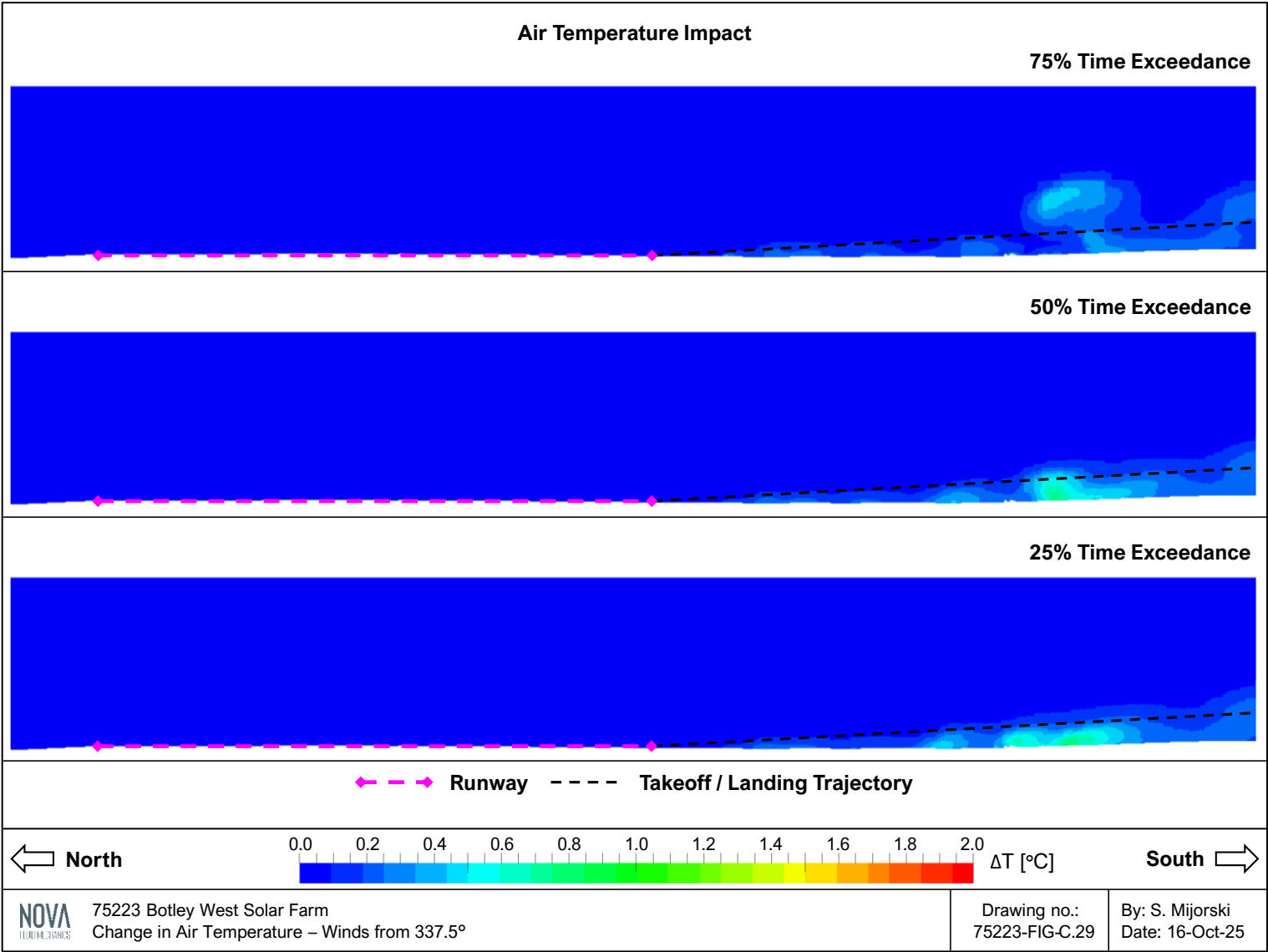


Figure C.30: Change in Mean Wind Speed – U-component – Winds from 337.5°

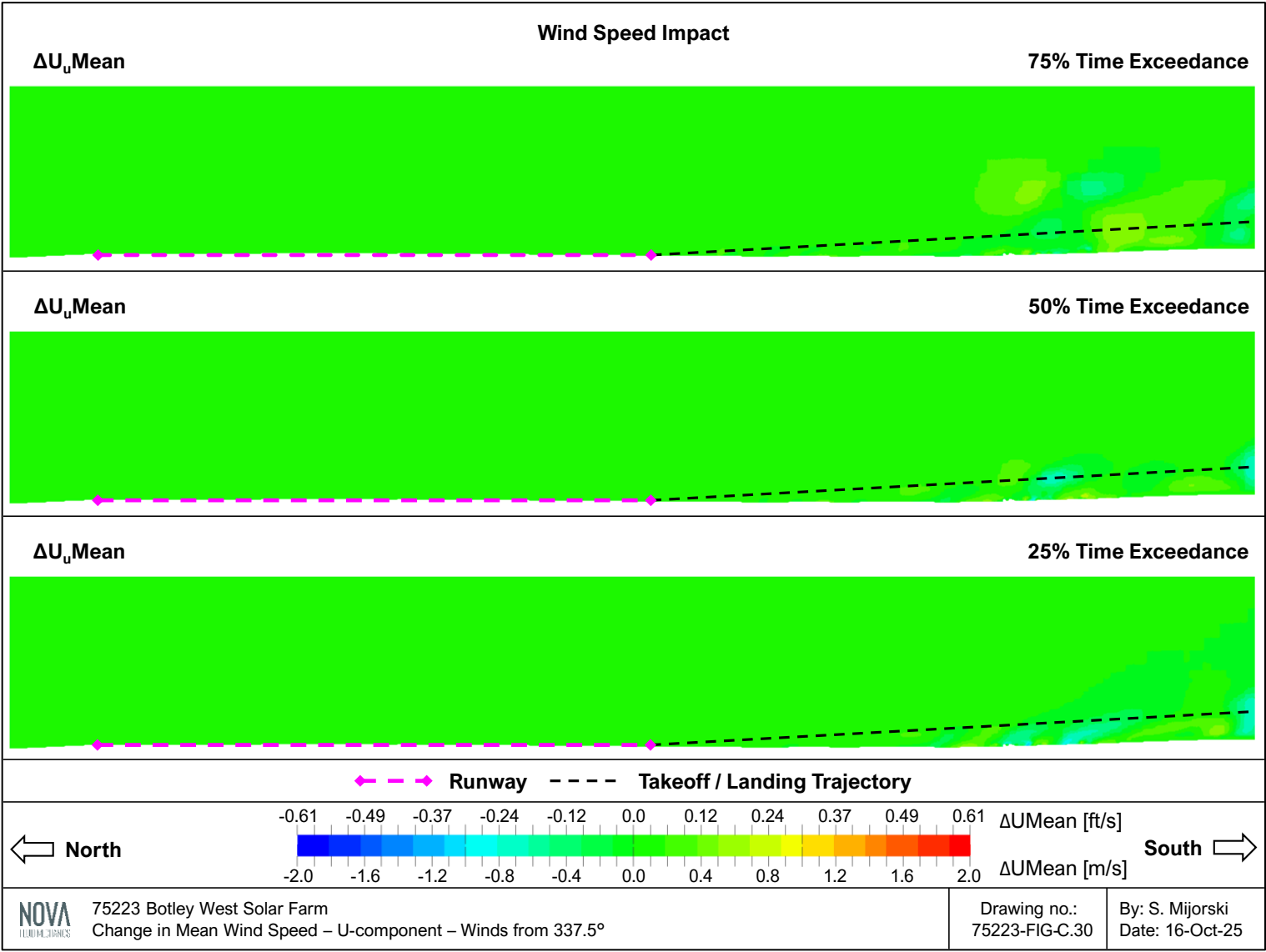


Figure C.31: Change in Mean Wind Speed – V-component – Winds from 337.5°

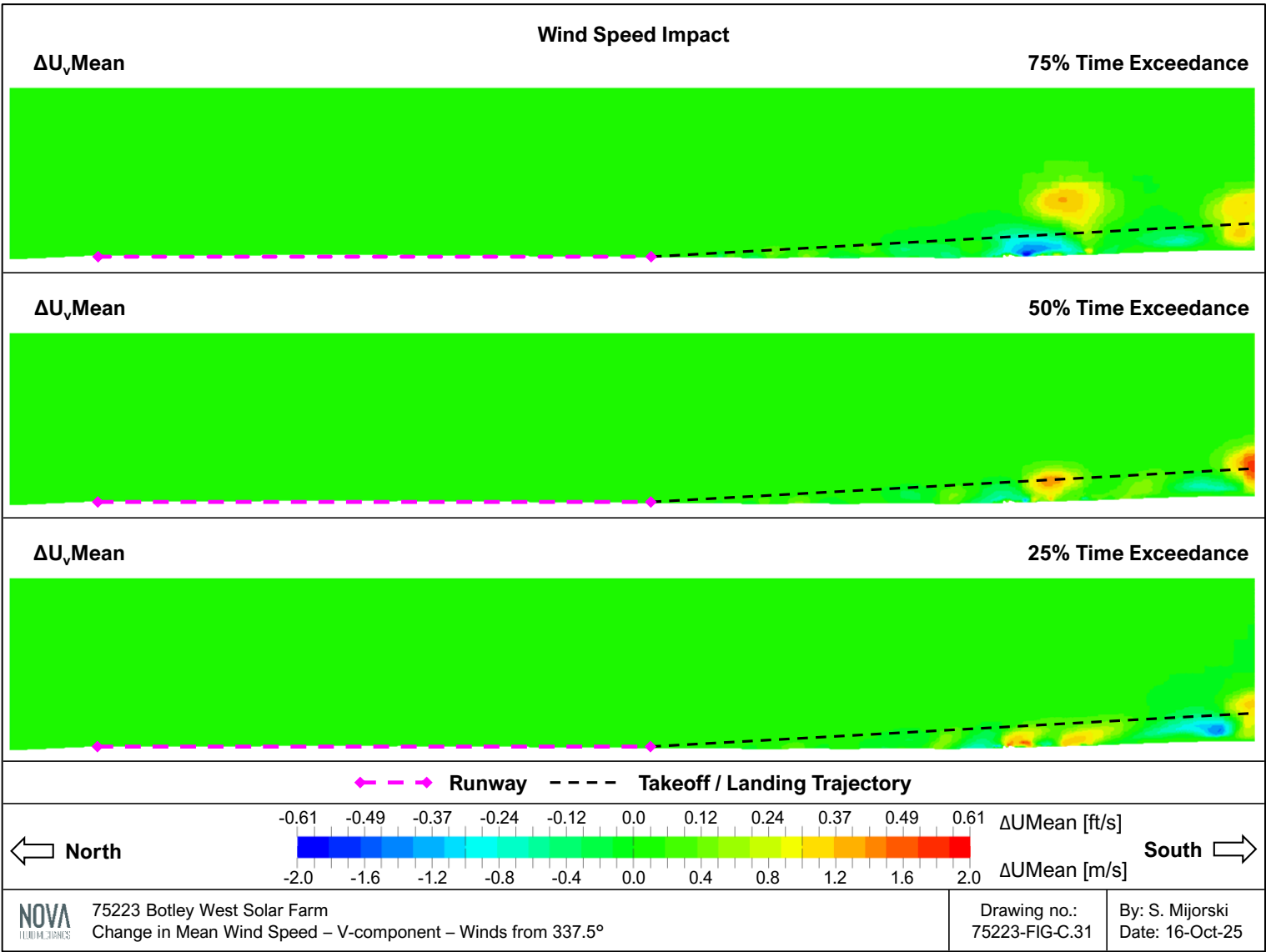


Figure C.32: Change in Mean Wind Speed – W-component – Winds from 337.5°

